

**EXHAUST GASES ENERGY RECOVERABLE FROM COMPRESSION IGNITION
ENGINE USING DIESEL AND BIODIESEL**

GEORGE ONYANGO ORIDO

A Thesis Submitted to the Graduate School in Partial Fulfilment for the Requirements of
Award of a Master of Science Degree in Agricultural Engineering of Egerton University


EGERTON UNIVERSITY

MARCH, 2018

DECLARATION AND RECOMMENDATION

Declaration

I declare that this thesis is my original work, and that it has not been wholly or in part presented for an award of any degree in any University known to me.

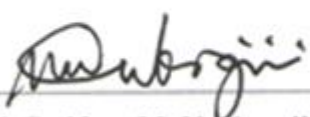
Signature:  Date: 02/03/2018

Name: **George Onyango Orido**

Reg. No: **BM11/41501/14**

Recommendation

This thesis is the candidate's original work and has been prepared with our guidance and assistance. It is presented for examination with our approval as official University Supervisors.

Signature:  Date: 03/03/2018

Name: **Prof. Godfrey M. N. Ngunjiri**

Department of Agricultural Engineering

Egerton University

Signature:  Date: 03/03/2018

Name: **Dr. Musa R. Njue**

Department of Agricultural Engineering

Egerton University

COPYRIGHT

© 2018 George Onyango Orido

This thesis is a copyrighted publication. No part of this publication may be reproduced by print, stored in a retrieval system or transmitted in any form or by any means: electrostatic, magnetic tape, mechanical, photocopying, recording or otherwise, without prior written permission from the author and/or Egerton University. All rights reserved.

DEDICATION

This thesis is dedicated to the late Professor Wilson Ogola who inspired and mentored me to get back to Egerton University and study Agricultural Engineering. I appreciate his moral support for he encouraged me to develop a positive attitude towards learning and he advised me on how to encounter challenges during my learning process.

ACKNOWLEDGEMENT

I thank God for the mercy, grace, guidance, protection, faithfulness, strength, good health and all the blessings that has led to success in education and other endeavours.

This was a further opportunity that I had to pursue my studies in the Department of Agricultural Engineering of Egerton University. It was as ever a challenge and an honour to study Engineering and be Prof. Ngunjiri's and Dr. Njue's student. Both had an understanding of their student, his learning and thinking process, and this is reflected in every page of this thesis.

I am thankful to Dr. Ngugi Kamau of the Faculty of Engineering and Technology in Egerton University, for his advice during proposal development. Distinguished gratitude goes to Prof. Nyaanga and Dr. Wambua Raphael all of the Department of Agricultural Engineering for their encouragement and advice during the thesis development. I thank the African Development Bank (AfDB) through the Ministry of Higher Education, Science and Technology (MoHEST) for the scholarship and financial support for the research. I appreciate the assistance of Mr. Waiyaki Erick of the School of Mechanical and Manufacturing Engineering in Jomo Kenyatta University of Agriculture and Technology, during data collection.

ABSTRACT

The broad objective of this research was to recover exhaust gases thermal energy from internal combustion engines for use in other applications. The specific objectives were: to determine the amount of thermal energy lost through exhaust gases at various engine speeds and loads; to determine the amount of energy recovered from exhaust gases at various engine speeds and loads; and to simulate the amount of maize that could be dried with the recovered energy. The experimental set-up consisted of a single cylinder, four-stroke, multi-fuel engine connected to an eddy current dynamometer for loading. Thermocouple temperature sensors and transmitters were used to measure exhaust gas to calorimeter inlet temperature and exhaust gas from calorimeter outlet temperature. Exhaust gas mass flow rate and temperature measurements were used to determine lost and recoverable energy. For purposes of estimating the amount of maize that could be dried with the recovered energy, safe and recommended temperatures were used. The dryer had a rated capacity of 1900 kg/h. The instrumentation of the engine was mainly equipped with a data acquisition system and ICE software. In general, fuel energy was observed to initially increase with engine speed and later decrease at higher speeds for both fuels at constant loads. For example, at 6 Nm fuel energy increased from 50295 kJ/h at 1000 rpm to 84945 kJ/h at 1250 rpm and later decreased to 64680 kJ/h at 1500 rpm for diesel fuel. The same trend was observed for biodiesel at a constant load of 6 Nm. At constant speeds, heat energy lost through exhaust gases increased with increased engine loading for both fuels. Recovered heat energy from exhaust gases increased with increased loading up to 18 Nm at speeds of 1000 rpm and 1250 rpm, but later decreased at a load of 22 Nm for both fuels. Heat energy could not be recovered at a speed of 1500 rpm and loads of 18 Nm and 22 Nm because calorimeter outlet temperatures of exhaust gases equaled inlet temperatures for both fuels. The specific energy required to dry maize from a moisture content of 25% to 13% wet basis was found to be 1124 kJ/kg. In this study, 750 and 566 grams per hour of maize could be dried through simulation when the engine used biodiesel and diesel respectively at an engine speed of 1000 rpm and a load of 18 Nm.

TABLE OF CONTENTS

DECLARATION AND RECOMMENDATION	ii
Declaration.....	ii
Recommendation.....	ii
COPYRIGHT	iii
DEDICATION.....	iv
ACKNOWLEDGEMENT.....	v
ABSTRACT.....	vi
TABLE OF CONTENTS	vii
LIST OF TABLES	x
LIST OF FIGURES	xi
SYMBOLS.....	xii
ABBREVIATIONS AND ACRONYMS.....	xiii
CHAPTER ONE	1
INTRODUCTION.....	1
1.1 Background Information.....	1
1.2 Statement of the Problem.....	4
1.3 Objectives	5
1.3.1 Main Objective.....	5
1.3.2 Specific Objectives	5
1.4 Research Questions.....	5
1.5 Justification.....	5
1.6 Scope.....	6

CHAPTER TWO	7
LITERATURE REVIEW	7
2.1 Operation Cycle of a Tractor Engine	7
2.1.1 Possibilities of Waste Heat Recovery on Tractor Engines	9
2.1.2 Engine Heat Recovery	11
2.2 Applications of Waste Heat	12
2.3 Engine Waste Heat Recovery Methods and Utilization	12
2.3.1 Direct Engine Waste Heat Recovery Method	12
2.3.2 Indirect Engine Waste Heat Recovery Methods	14
2.3.3 Waste Heat for Refrigeration Purposes.....	17
2.3.4 Waste Heat for Mechanical Turbo-compounding Purposes	18
2.4 Waste Heat Recovery Benefits	19
2.5 Air as a Drying Fluid	19
2.6 Summary of the Reviewed Literature	20
CHAPTER THREE	22
MATERIALS AND METHODS	22
3.1 Experimental Set-up.....	22
3.2 Data Collection	22
3.3 Fuel Energy	23
3.4 Heat Lost through Exhaust.....	24
3.5 Heat Energy Recovered	24
3.6 Grain Drying Models	25
CHAPTER FOUR.....	27
RESULTS AND DISCUSSIONS.....	27
4.1 Thermal Energy Lost through Exhaust	27
4.2 Heat Energy Recovered	33

4.3 Maize Drying Simulation.....	39
CHAPTER FIVE	43
CONCLUSIONS AND RECOMMENDATIONS.....	43
5.1 Conclusions.....	43
5.2 Recommendations.....	44
REFERENCES.....	45
APPENDICES	54

LIST OF TABLES

Table 2. 1: Various engines and their output	11
Table 4. 1: Fuel energy (kJ/h) for different engine speeds and torque loads.....	28
Table 4. 2: Heat energy (kJ/h) lost through exhaust for different engine speeds and torque loads	28
Table 4. 3: Exhaust gas to calorimeter average inlet temperature (°C) for different engine speeds and torque loads	32
Table 4. 4: Recovered heat energy (kJ/h) for different engine speeds and torque loads	33
Table 4. 5: Exhaust gas from calorimeter outlet temperature (°C) for different engine speeds and torque loads	38
Table 4. 6: Maize drying potential (g/h) for different engine speeds and torque loads	41

LIST OF FIGURES

Figure 1. 1: Mechanized grain dryer.....	4
Figure 2. 1: Sample of load factor evolution of a simulation on-field operation cycle	8
Figure 2. 2: Total fuel energy distribution in an internal combustion engine.....	10
Figure 2. 3: Thermoelectric generator	13
Figure 2. 4: Rankine cycle	15
Figure 2. 5: Vapour absorption cycle.....	17
Figure 2. 6: Turbocharger	19
Figure 3. 1: Research engine test setup.....	23
Figure 4. 1: Heat energy lost through exhaust against torque load at 1000 rpm	29
Figure 4. 2: Heat energy lost through exhaust against torque load at 1250 rpm	30
Figure 4. 3: Heat lost through exhaust against torque load at 1500 rpm	31
Figure 4. 4: Recovered energy against torque load at 1000 rpm	35
Figure 4. 5: Recovered energy against torque load at 1250 rpm	37
Figure 4. 6: Recovered energy against torque load at 1500 rpm	38
Figure 4. 7: Estimated maize that could be dried against torque load at 1000 rpm.....	41
Figure 4. 8: Estimated maize that could be dried against torque load at 1250 rpm.....	42
Figure 4. 9: Estimated maize that could be dried against torque load at 1500 rpm.....	42

SYMBOLS

Symbol	Description
CO	Carbon monoxide
CO ₂	Carbon dioxide
HC	Hydrocarbons
NO _x	Oxides of Nitrogen

ABBREVIATIONS AND ACRONYMS

Abbreviation/Acronym	Description
CI	Compression Ignition
DOC	Diesel Oxidation Catalyst
ETEG	Exhaust Based Thermoelectric Generator
ICE	Internal Combustion Engine
ORC	Organic Rankine Cycle
PM	Particulate Matter
PTO	Power Take Off
rpm	Revolutions Per Minute
UDDS	Urban Dynamometer Driving Schedule
VCR	Variable Compression Ratio
VVT	Variable Valve Timing
WHR	Waste Heat Recovery
WHRS	Waste Heat Recovery System

CHAPTER ONE

INTRODUCTION

1.1 Background Information

The diesel engine is the most efficient of all internal combustion engines with compression ratios ranging from 14 to 16 compared to spark ignition engines with compression ratios ranging from 10 to 12 (Lloyd & Cackette, 2001). It achieves this high level of performance by compressing air to high pressures before injecting very small droplets of fuel into the combustion chamber. The high temperatures created when air is highly compressed in a diesel engine make the fuel to burn without the spark plug required in a spark ignition engine. Large diesel engines, which are used for stationary power production and to power boats and ships, can be twice as efficient as a conventional automobile spark ignition engine. However, according to (Heywood, 1988) the high pressures created inside diesel engines make heavy engines with thick cylinder walls necessary. Diesel engines have been useful for trucks, buses, small and medium-size ships and tugs, movable industrial-power systems, and diesel-electric railroad locomotives. They have been unsuitable for use in aircraft, and have found only limited acceptance in passenger automobiles. Diesel engines use a conventional cylinder and piston arrangement. The cylinders may be arranged vertically in line, in two banks forming a V, or horizontally opposing each other (Ganesan, 2012)

Internal combustion engines are the greatest consumers of fossil fuel in the world (Van der Hoeven, 2012). From the total heat supplied to the engine in the form of fuel, approximately, 30 to 40% is converted into useful mechanical work. The heat which remains is expelled through exhaust gases to the environment and engine cooling systems, resulting in serious environmental pollution (Ban-Weiss *et al.*, 2008). With research on waste heat recovery of exhaust gas from internal combustion engines, energy supply will be increased and the impact of global warming due the emission of carbon dioxide would be reduced. Exhaust gases immediately leaving the engine can have temperatures as high as 450-600°C (Jadhao & Thombare, 2013). It is imperative that effort should be launched for conserving energy through exhaust heat recovery techniques. Such a waste heat recovery technique would ultimately reduce the use of conventional fossil fuel energy. The internal combustion engine has been a primary power source for automobiles over the past century. Presently, high fuel costs and concerns about foreign oil dependence have resulted in increasingly complex engine designs to decrease fuel consumption. For example, engine manufacturers have implemented techniques such as enhanced fuel-air mixing, turbo-charging, and variable

valve timing in order to increase thermal efficiency. However, around 60-70% of the fuel energy is still lost as waste heat through the coolant and the exhaust (Gotmalm, 1992). Moreover, increasingly stringent emissions regulations are causing engine manufacturers to limit combustion temperatures and pressures lowering potential efficiency gains (Endo *et al.*, 2007). It is argued that the engine has consumed more than 60% of fossil oil, as the most widely used source of primary power for machinery, critical to the transportation, construction and agricultural sectors (Stoss *et al.*, 2013). On the other hand, legislation of exhaust emission levels has focused on carbon monoxide (CO), hydrocarbons (HC), nitrogen oxides (NO_x), and particulate matter (PM). Energy recovery on engine exhaust is one of the ways to deal with these problems since it can improve the energy utilization efficiency and reduce emissions (Gopal *et al.*, 2010). Given the importance of increasing energy conversion efficiency for reducing both the fuel consumption and emissions of internal combustion engines, scientists and engineers have done lots of successful research aimed at improving engine thermal efficiency, including supercharge and lean mixture combustion. However, in all the energy saving technologies studied, engine exhaust heat recovery has been less emphasized.

Many researchers recognize that waste heat recovery from engine exhaust has the potential to decrease fuel consumption thereby decreasing greenhouse gas emissions, and recent technological advancements have made these systems viable and cost effective (Özcan & Söylemez, 2006; Rahman *et al.*, 2013; Will, 2010). Among the different technologies available for waste heat recovery (WHR) applications to internal combustion engines (ICEs), the Rankine cycle is traditionally regarded as one of the solutions (Armstead & Miers, 2014). Extensive work has been proposed in relation to the application of Rankine cycles in road transport (Shokati *et al.*, 2014), as well as in the maritime sector (Kalikatzarakis & Frangopoulos, 2015). Road and maritime applications normally differ markedly in terms of their operating conditions. Waste heat recovery system (WHRS) design for application in international shipping focuses on steady state conditions, and often, on one individual operating point, due to typically stationary operations of such systems. On the other hand, road applications require focus on transient operations, which leads to the existence of extensive literature on WHR control systems (Feru *et al.*, 2013; Quoilin *et al.*, 2011). Even in the latter case, however, although observations from real operations are sometimes used to weight the selected operating points (Espinosa *et al.*, 2010), the WHRS design still relies on steady state methods. Heating and cooling periods are sometimes considered (Lee *et al.*,

2014) but this is mainly done in order to estimate the time of response rather than for optimising the heat recovery potential. Non-road machinery, particularly agricultural machines, and inland shipping vessels constitute a significant share of respectively land and sea based transportation. These vehicles generally follow clearly identifiable operating cycles which are significantly dynamic but follow a determinate, repeatable pattern. In addition, compared to cars and trucks, these applications show higher engine load coefficient and exhaust gas temperatures (Espinosa *et al.* (2010); Hsiung & Yeh, 2014; Lacour *et al.*, 2011; Nielsen *et al.*, 2014). Hence, being in between steady state generator and heavy transient road engines for both size and transient behaviour, heavy non road engines (marine or agriculture) should have specifically designed heat recovery systems (Ringler *et al.*, 2009). Several studies are dedicated to the dynamic performance of single phase heat exchangers as well as to two-phase ones (Feru *et al.*, 2014; Morales *et al.*, 2012; Quoilin *et al.*, 2011). However, the subject of efficient designs of WHRS evaporator based on dynamic cycle performance still remains unclear.

According to Magan and Aldred (2007), grain will normally be harvested at a moisture content of 18% to 25% wet basis, although it can be substantially higher or lower depending on many factors such as the stage of maturity, season, weather pattern and drying facilities. With good ventilation through the store, the grain can be harvested just after it is ripe (around 30% moisture content for maize) but most drying methods allow some of the drying to take place naturally while the crop is still standing in the field. For maize, the tradition in most parts of Kenya is to leave the crop in the field until the moisture content has fallen to around 18%. When the moisture content of the produce reaches equilibrium with the humidity of the ambient air, drying will stop. Maize will dry down to approximately 13% moisture content. Mechanized dryers are used to dry maize grain in large quantities. They are recirculating batch, cross-flow grain dryers with axial fans, propane burners and cylindrical grain chambers enclosing their air plenums. Figure 1.1 illustrates the various parts of a mechanized grain dryer. The grain is fed into the bottom of a vertical auger by the grain agitator and continuously recirculated from the bottom to the top of the dryer. Outside air is forced by the fan past the burner into the air plenum and through the grain chamber, to dry the grain. The dryer is power take-off driven by a stationary tractor. Practically all modern tractors use diesel engines.

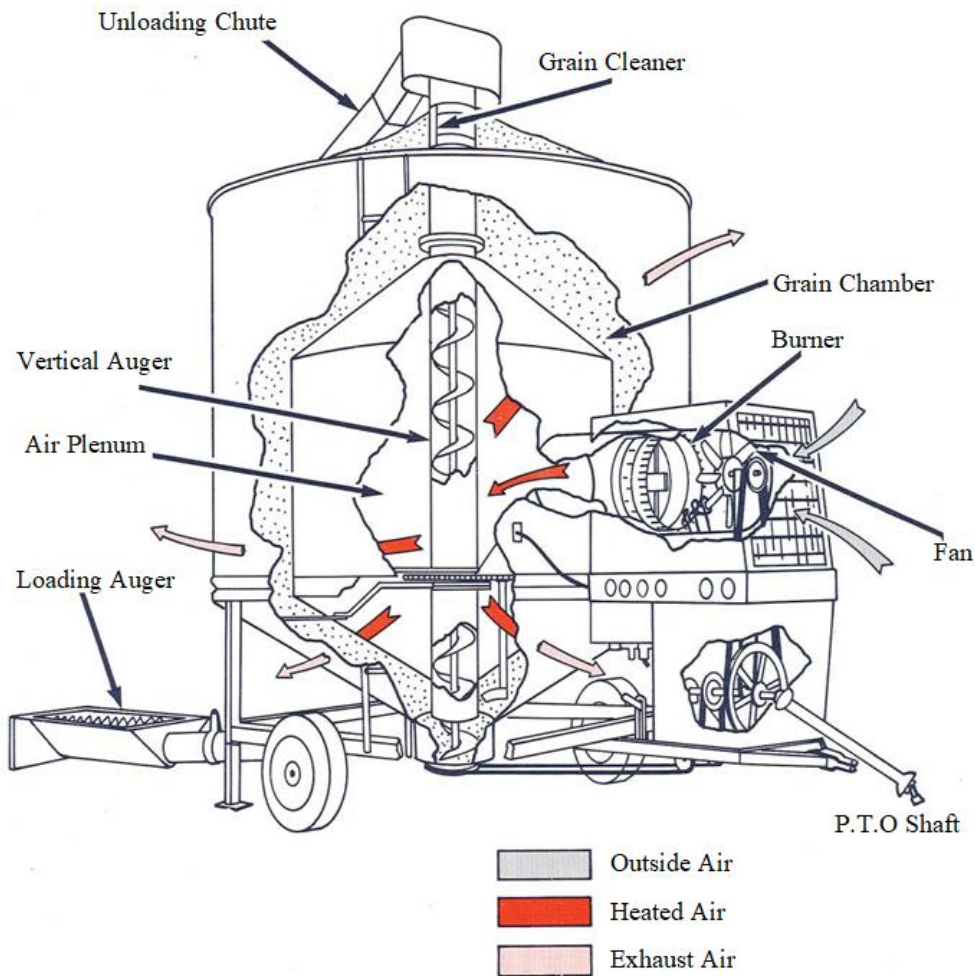


Figure 1. 1: Mechanized grain dryer

(Source: Alberta Farm Machinery Research Centre, 1983)

1.2 Statement of the Problem

Despite the high level of development of the engine systems and controls, the maximum efficiency of 40% is reached in certain operation points; most of the time, engines run with efficiencies of 15% to 35%. It means that more than 60% of the fuel energy is lost. About 30% of the lost energy is in form of heat in the exhaust system. The expelled heat results into undesirable entropy rise in the environment. There is need therefore to develop strategies to recover the waste energy.

1.3 Objectives

1.3.1 Main Objective

The main objective of this research was to recover exhaust gases energy from internal combustion engines for use in other applications.

1.3.2 Specific Objectives

The specific objectives were:

- i. To determine the amount of heat energy lost through the exhaust gases at various engine speeds and torque loads.
- ii. To recover heat energy from the exhaust gases at various engine speeds and torque loads.
- iii. To estimate the amount of maize that could be dried with the recovered heat energy from 25% to 13% moisture content on wet basis.

1.4 Research Questions

- i. How much heat energy is lost through the exhaust gases at various engine speeds and torque loads?
- ii. How much heat energy is recovered from the exhaust gases at various engine speeds and torque loads?
- iii. How much maize could be dried with the recovered heat energy from 25% to 13% moisture content on wet basis?

1.5 Justification

To address the problem of heat energy loss in engines especially through the exhaust gases, there is need for research on energy recovery and subsequent utilization. Moreover, studies on total energy distribution from an internal combustion engine have shown that out of the possible 100% fuel energy content in an engine, 35% is useful as brake power, 30% is lost in the cooling system, 5% is lost through radiation and approximately 30% is lost through the engine exhaust (Jadhao & Thombare, 2013). Use of the recovered exhaust energy in applications such as maize drying would be beneficial in a number of ways: propane heating costs associated with the dryer is minimized; and contact with dangerous propane is avoided thus, solving the propane handling challenge — operators of the dryer have to wear rubber gloves and eye protection while connecting the rubber hose to liquid propane.

1.6 Scope

This research was limited to the recovery of energy only from the exhaust gases of a four stroke cycle engine. The recovered energy was used to estimate the amount of maize that could be dried from a moisture content of 25% to 13% wet basis. The research did not cover heat recovery from the cooling system which was another major route for heat loss (about 30%) from an internal combustion engine.

CHAPTER TWO

LITERATURE REVIEW

2.1 Operation Cycle of a Tractor Engine

Tractors have many applications but their operation can be divided into two regimes: transportation and work in the fields. In the fields the tractor runs with constant speed from one to the other side of the field then it takes some time to turn at the end of the field. This cycle is repeated many times as shown in Figure 2.1. The constant speed of the tractor means that the engine runs at an almost constant load. The fuel consumption, engine power, engine efficiency and the enthalpy of the exhaust gases are constant. According to (Punov *et al.*, 2013), the constant quantity of waste energy is produced during 80% of the time when the tractor works in the fields. Milkov *et al.* (2014) demonstrated that the energy balance can be made through a comparison between: the energy put in with the fuel, the energy converted in the effective power, the energy lost through friction, the energy lost in the cooling system and the energy lost with exhaust gases. The energy of the exhaust gases is calculated by the enthalpy which goes out from the cylinders through the exhaust valves.

As in every technical application, diesel engines for agricultural machinery have their own typical features which have to be well known in order to understand the issues they are connected to. The most typical feature of a tractor is the fact that, in several applications, power consumption is not strictly related to tractor displacement. It was experimentally demonstrated by (Grasso *et al.* (2007)) that during working operation most of power absorption is related to the working equipment pulled by the tractor. This is possible, thanks to a second shaft, directly connected to the engine and coaxial with tractor shaft, that transfers mechanical energy from the engine to the agricultural equipment. The two shaft movements are normally independent, which means that it is possible for the tractor to move while the equipment is not working, as well as the latter to do his job while the tractor is not moving (Schumacher *et al.*, 1991). The shaft connection between the tractor and its equipment is called power take off (PTO). This feature is important in order to understand engine's transient behavior. One of tractors' specific features is, in fact, their particular kind of transient operations. Tractors are generally used alternatively for two different goals, each having its specific features: on the field, for pulling and giving energy to agricultural equipment and on the road or on the field, for transporting goods. The main difference lies in load factor variation with time as demonstrated by Palmer *et al.* (2003). Normal operations of agricultural machines on the field involve a periodical variation for engine load: full-load

operation, when tractor is moving with its equipment working and partial-load operation, typically in maneuvering operations, when equipment is not working.

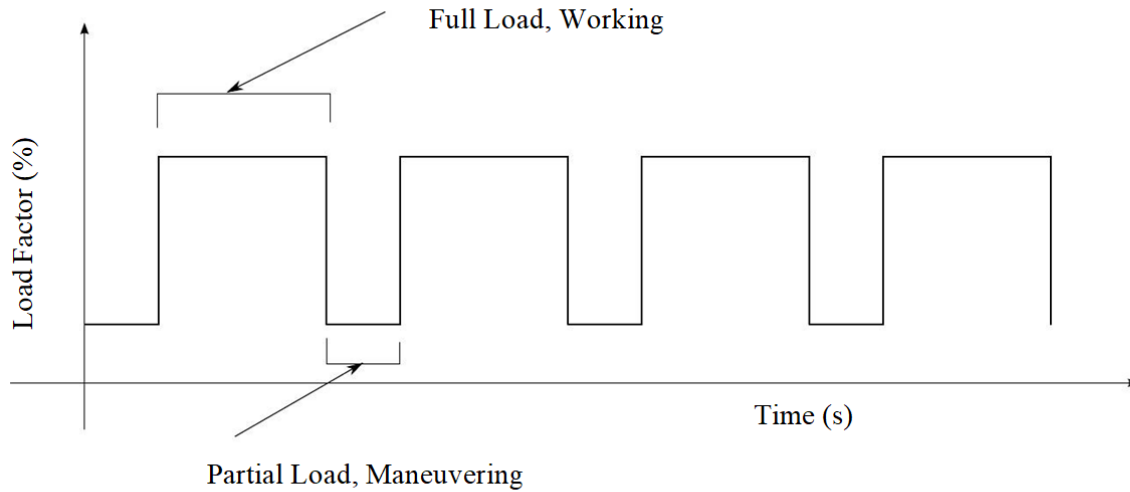


Figure 2. 1: Sample of load factor evolution of a simulation on-field operation cycle

Source: Punov *et al.* (2013)

Figure 2.1 however, is not a completely veritable representation. In fact, even if full load conditions are well represented by a constant load behavior, the same cannot be said for maneuvering operations, where evidence is shown of an unsteady and unpredictable behaviour. Concerning road transportation, load behavior is more variable and similar to that of cars. Kadota and Yamamoto (2008) are of the opinion that the two different components of standard real life operations can mix in very different ways depending on several variables such as field dimensions, and kind of crop. These features make agricultural machines behavior in transient operation very different from other applications employing diesel engines, such as cars, trucks, ships and trains. This reasoning leads to the idea that diesel steady state behavior does not change dramatically between different applications; this being mainly related to some general features that could normally make it possible to compare car, truck and tractor engines. The typical features in real life operations are what really make the difference, involving variable load conditions and a strong influence of transient behavior. Edwards *et al.* (2010) emphasized the importance of transient impact knowledge on waste heat recovery potential in order to make a correct choice of all system parameters.

2.1.1 Possibilities of Waste Heat Recovery on Tractor Engines

Sathiamurthi (2011) concluded that waste heat is heat, which is generated in a process by way of fuel combustion or chemical reaction, and then “dumped” into the environment even though it could still be reused for some useful and economic purpose. This heat depends in part on the temperature of the waste heat gases and mass flow rate of exhaust gas (Kruiswyk, 2008). Waste heat losses arise both from equipment inefficiencies and from thermodynamic limitations on equipment and processes (Moran *et al.*, 2010). For example, for an internal combustion engine; approximately 30 to 40% of the heat is converted into useful mechanical work. The remaining heat is expelled to the environment through exhaust gases and engine cooling systems. It means approximately 60 to 70% energy is waste heat through exhaust and the cooling system

Exhaust gases immediately leaving the engine can have high temperatures and high mass flow rate. Consequently, these gases have high heat content, carried away as exhaust emission. Efforts can be made to design more energy efficient engine with better heat conversion to useful work and lower exhaust gas temperatures; however, the laws of thermodynamics place a lower limit on the temperature of exhaust gases (Karellas *et al.*, 2013). Figure 2.2 shows the total energy distribution from an internal combustion engine. In automobile engines significant amount of heat is released to the environment. For example, As much as 35% of the thermal energy generated from combustion in an automotive engine is lost to the environment through exhaust gas and other losses (Hatazawa *et al.*, 2004).

Diesel engines have a wide field of applications as discussed in (Baldia *et al.*, 2015). They are characterized by their high efficiency as energy converters. Small air cooled diesel engines of up to 35 kW output are used for irrigation purposes, as small agricultural tractors and as construction machines. Large farms employ tractors of up to 150 kW output. Water or air cooled engines are used for a range of 35-150 kW and unless an air cooled engine is strictly required, water cooled engines are preferred for higher power ranges. Earth moving machinery uses engines with an output of up to 520 kW or even higher, up to 740 kW. Marine and locomotive applications usually employ engines with an output range of 150 kW or more (Kalligeros *et al.*, 2003). Trucks and road engines usually use high speed diesel engines with 220 kW output or more. Diesel engines are used in small electrical power generating units or as standby units for medium capacity power stations (Hossain & Bari, 2011).

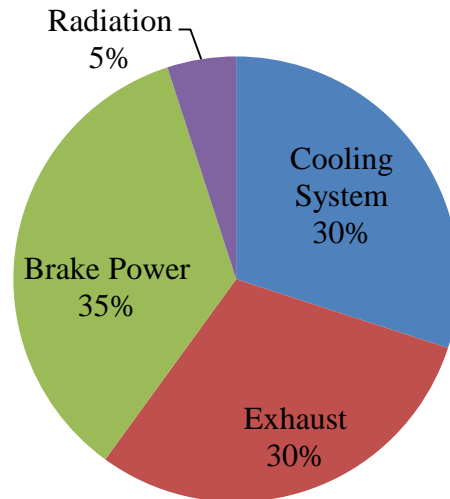


Figure 2. 2: Total fuel energy distribution in an internal combustion engine
(Adapted from Jadhao & Thombare, 2013)

In general, diesel engines have efficiency of about 35% and thus the rest of the input energy is wasted. Despite recent improvements of diesel engine efficiency, a considerable amount of energy is still expelled to the ambient with the exhaust gas. Table 2.1 shows various engines and their output. In a water-cooled engine of about 35 kW, 30-40% of the input energy is wasted in the coolant and exhaust gases each. The amount of such loss, recoverable at least partly, greatly depends on the engine load. Johnson (2002) found that for a typical 3.0 liters engine with a maximum output power of 115 kW, the total waste heat dissipated can vary from 20 kW to as much as 40 kW across the range of usual engine operation. It is suggested that for a typical and representative driving cycle, the average heating power available from waste heat is about 23 kW, compared to 0.8–3.9 kW of cooling capacity provided by typical passenger car variable compression ratio (VCR) systems (Nam, 2000). Since the wasted energy represents about two-thirds of the input energy and for the sake of a better fuel economy, exhaust gas from internal combustion engines can provide an important heat source that may be used in a number of ways to provide additional power and improve overall engine efficiency (Conklin & Szybist, 2010). These technical possibilities are currently under investigations by research institutes and engine manufacturers. For the heavy duty automotive diesel engines, one of the most promising technical solutions for waste heat from exhaust gas use appears to be utilization into useful work.

Table 2. 1: Various engines and their output**(Source: Hossain & Bari, 2011)**

Serial Number	Engine Type	Power Output (kW)	Waste Heat
1	Small Air Cooled Diesel Engines	35	
2	Small Agricultural Tractors and Construction Machines	150	30-40% of Energy Waste from I.C. Engine
3	Water or Air Cooled Engines	35-150	
4	Earth Moving Machines	520-720	
5	Marine Applications	150-220	
6	Trucks and Road Engines	220	

2.1.2 Engine Heat Recovery

Large quantity of hot flue gases is generated from internal combustion engines. If some of this waste heat could be recovered, a considerable amount of primary fuel could be saved. It depends upon mass flow rate and temperature of exhaust gas (Hounsham *et al.*, 2008). The internal combustion engine energy lost in waste gases cannot be fully recovered. However, much of the heat could be recovered and losses be minimized by adopting certain measures. The mass flow rate of exhaust gas is a function of the engine size and speed, hence the larger the engine size and the higher the speed, the more the exhaust gas heat. So heat recovery system will be beneficial to the large engines as compared to smaller engines. According to Daccord *et al.* (2013) heat recovery from exhaust gas and conversion in to mechanical power is possible with the help of Rankine, Stirling and Brayton thermodynamic cycles. These cycles are recommended for low temperature heat conversion to useful power. Engine exhaust heat recovery is considered to be one of the most effective means of heat conversion to useful power and it has become a research hotspot recently (Nelson, 2008). Recovering engine waste heat can be achieved via numerous methods. The heat can either be reused within the same process or transferred to another thermal, electrical, or mechanical process. Literature review shows that the highest potential of recovery is in the heat of the exhaust gases (Leduc & Smague, 2013). In some engines the exhaust gases heat is used for heating the cooling system during the warm up period. It accelerates the warming up of the engine.

2.2 Applications of Waste Heat

According to Shahadat *et al.* (2005), waste heat can be utilized for applications like space heating and preheating intake air. Herner *et al.* (2009) investigated the effect of preheating intake air on NO_x emission on diesel engine. A waste heat recovery system for preheating intake air was designed and fabricated, and its effect was tested on diesel combustion and exhaust emissions. Results showed that NO_x emission reduced with intake preheating. Higher inlet air temperature lowered ignition time which was responsible for lower NO_x formation. Uniform or better combustion occurred due to preheating of inlet air resulting in lower engine noise. Easy vaporization and better mixing of air and fuel occurred due to warm up of inlet air, which caused lower CO emission. Low grade fuel, such as, kerosene can be used in diesel engine by blending with conventional diesel fuel (Bhale *et al.*, 2009). Using the air preheating system and 10% kerosene blend as fuel, the thermal efficiency is improved and exhaust emissions (NO_x and CO) are reduced as compared to only diesel fuel without using air preheating system. Karaosmanoglu (1999) concluded that use of alternative fuel in internal combustion engines leads to some problems such as poor fuel atomization and low volatility. The problems mainly originated from their high viscosity, high molecular weight and density. It is reported that these problems may cause important engine failures such as piston ring sticking, injector coking, formation of carbon deposits and rapid deterioration of lubricating oil after the use of alternative fuel for a long period of time. Waste heat recovery is useful for preheating alternative fuel so as to reduce the viscosity of fuel, make fuel atomization better and lower the volatility of fuel. Temos (2006) demonstrated that waste heat can be utilized indirectly for power generation using the Rankine cycle, Brayton cycle, and Stirling cycle. Research has shown that waste heat can be used directly for thermoelectric generation, piezoelectric generation, thermionic generation, and thermo photo-voltaic. Thermo photo-voltaic specifically converts radiant energy into electricity.

2.3 Engine Waste Heat Recovery Methods and Utilization

2.3.1 Direct Engine Waste Heat Recovery Method

In this method power generation from waste heat typically involves waste heat utilization from internal combustion engine to generate mechanical energy that drives an electric generator. Electricity generation is directly from a heat source such as thermoelectric and piezoelectric generator (Enderlein *et al.*, 2005). The factor that affects power generation is thermodynamic limitations for different temperature range. The efficiency of power

generation is heavily dependent on the temperature of the waste heat gas and mass flow rate of exhaust gas. In thermoelectric generation the exhaust pipe contains a block with thermoelectric materials that generates a direct current, thus providing at least some of the electric power requirements in which two different semiconductors are subjected to a heat source and a heat sink, Yuchao *et al.* (2013), thereby creating a voltage between two conductors. It is based on the seebeck effect. The cooling and heating is done by applying electricity. The efficiency is low, approximately 2 to 5% and the cost is high (Xiaodong & Chau, 2011). Figure 2.3 shows a thermoelectric generator and its components. Advantages of a thermoelectric generator include; free maintenance, silent operation, and high reliability. It is compact, environmentally friendly and involves no moving and complex mechanical parts. Because of these merits, it is presently becoming a noticeable research direction. Recycling and reusing waste exhaust gas can not only enhance fuel energy use efficiency, but also reduce air pollution (Vázquez *et al.*, 2002). Thermal power technology such as the thermoelectric generator raises, therefore, significant attention worldwide. Research has been carried out on thermoelectric generator devices using the exhaust gas of vehicles as heat source, and preliminary analysis of the impact of relevant factors on the output power and efficiency of the devices (Acharyaviriya *et al.*, 2000). The work simulated the impact of relevant factors, including vehicles exhaust mass flow rate; temperature and mass flow rate of different types of cooling fluid; convection heat transfer coefficient; height of P-type and N-type semiconductor; the ratio of external resistance to internal resistance of the circuit on the output power and efficiency.

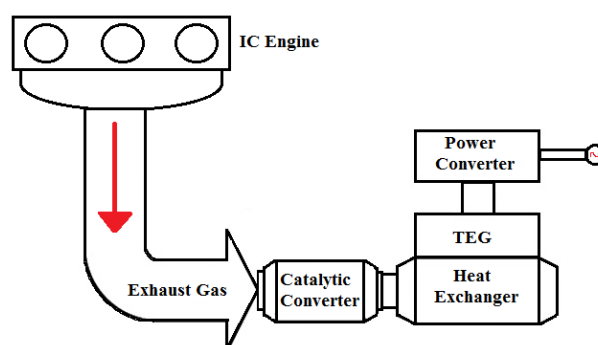


Figure 2. 3: Thermoelectric generator
(Source: Jadhao & Thombare, 2013)

The results showed that the output power and efficiency increased significantly by changing the convection heat transfer coefficient of the high temperature-side than that of low-temperature-side. Pilot program was made to investigate the applicability of

thermoelectric generators to the recovery of medium temperature waste heat from a low power stationary diesel engine. Studies showed the optimum operating conditions to achieve maximum power outputs from the waste heat recovery system (Haidar & Ghajel, 2001). A similar study on waste heat recovery system by using thermoelectric generator from internal combustion engine reviewed the main aspects of thermal design of exhaust based thermoelectric generator (ETEG) systems (Saqr *et al.*, 2008). Analysis of a thermoelectric generator for power generation from internal combustion engine showed results as 20% of energy releasing potential for the waste heat from engine. It was able to release 30-40% of the energy supplied by fuel depending on engine load (Chauhan, 2012). Piezoelectric generation is used for low temperature ranges of 100°C to 150°C. According to McMeeking (2004), piezoelectric devices convert mechanical energy in the form of ambient vibration to electric energy. It is usually in the form of a thin film membrane which can take advantage of oscillatory gas expansion to create a voltage output (Shindo *et al.*, 2002). Thermionic generator is a thermoelectric device operating on thermionic emission. In this system, a temperature difference drives the flow of electron through vacuum from metal to metal oxide surface at 1000°C. Thermo photo-voltaic converts radiant energy to electricity (Wang & Zhang, 2004). Heating of emitter emits electromagnetic radiation. All direct electric conversion devices have low efficiency which can be increased by technology. Advantages in alternate power cycle may increase feasibility of power generation at low temperature. This direct method of power generation device is high in cost and low in efficiency as reported by (Xuyue & Yu, 2001). It can be easily handled, compact in size and require minimum space.

2.3.2 Indirect Engine Waste Heat Recovery Methods

The Rankine cycle is a system based on the steam generation in a secondary circuit using the exhaust gas thermal energy to produce additional power by means of a steam expander (Espinosa *et al.*, 2010). A special case of low temperature energy generation systems uses certain organic fluids instead of water commonly known as organic Rankine cycle (Quoilin *et al.*, 2012). This technique has the advantage compared with turbo-compounding that does not have an important impact on the engine pumping losses and with respect to thermoelectric materials that provides higher efficiency in the use of the residual thermal energy sources. Waste heat recovery from Rankine cycle operated at low temperature difference using unconventional fluids (refrigerants, CO₂, binary mixtures) is shown in Figure 2.4. At very low heat source temperatures, the trans-critical CO₂ cycle produces the highest net power output (Galanis *et al.*, 2009). Rankine bottoming cycle techniques

maximize energy efficiency; reduce fuel consumption and greenhouse gas emissions (Srinivasan *et al.*, 2010). Recovery of engine waste heat is achieved using working fluids. Waste heat recovery from an internal combustion engine was analysed with two different fluids by using organic Rankine cycle. The best performance was obtained when the hydrochlorofluorocarbon, R-123 was applied as the working fluid. The heat can either be reused within the same process or transferred to another thermal, electrical, or mechanical process (Saidur *et al.*, 2012). Investigation and market evaluation of organic Rankine cycle can be applied in several cost effective areas. Analysis shows that evaporator pressure gives better efficiencies. Pinch point temperatures, heat exchangers' cost, and critical temperature of working fluid would be a restriction for maximum working pressure of the cycle. Organic Rankine cycles like in combined heat and power units are options to improve total engine fuel efficiency and reduce cost (Drescher & Brüggemann, 2007). Waste heat recovery using organic Rankine cycle is a an efficient method compared with the other techniques; so automobile manufacturers use this method to enhance the efficiency of their products (Kumar *et al.*, 2011). The economic feasibility of waste heat recovery from diesel engine exhaust gas and analysis of harmfulness of the gases was done by using the methods of purification and processing diesel engine exhaust gas as reported by (Seher *et al.*, 2012). A computational model was developed which determined diesel exhaust emission rate, diesel exhaust waste heat rate and useful results for the diesel engine were found. Heat recovery was done and it increased with increasing exhaust mass flow rate (Xuejun & Peng, 2012).

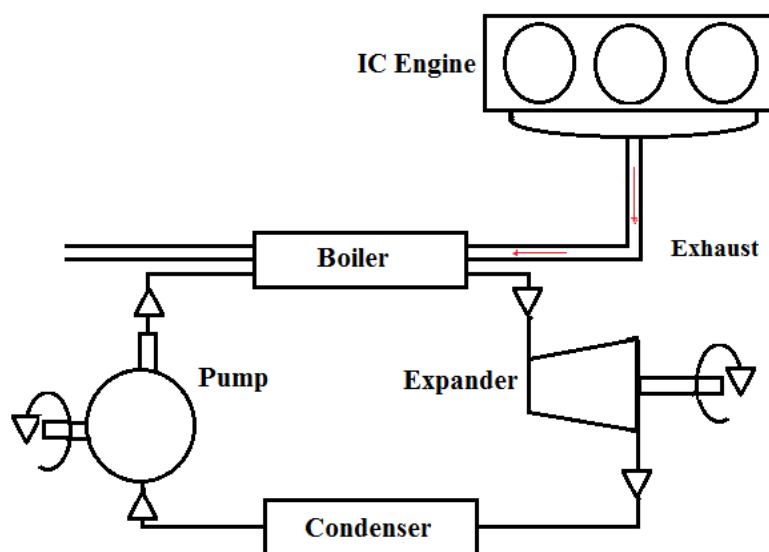


Figure 2. 4: Rankine cycle

(Source: Jadhao & Thombare, 2013)

The Stirling cycle as an indirect waste heat recovery method is a thermodynamic cycle that describes the general class of Stirling devices which includes the Stirling engine. A Stirling engine is a heat engine operating by cyclic compression and expansion of air or other gas as the working fluid at different temperature levels such that there is a net conversion of heat energy to mechanical work (Zulkifli *et al.*, 2008). Linearly reciprocating internal combustion engine offers many advantages over the conventional crank-slider engine. Benefits include improved efficiency, higher power-to-weight ratio and multiple fuel capability. Developments of gamma type Stirling engines which operate at high temperature differences were advanced to find out the optimum temperature difference at which the model would give maximum thermal efficiency (Kong *et al.*, 2004).

The observed reduction of fuel consumption was also studied (Wu & Wang, 2006). A free piston Stirling engine was designed with its key techniques. Key issues while designing a free piston Stirling engine were analysed during waste heat recovery. A set of free piston Stirling engines with output power, hot and cold space temperatures and operation frequencies were designed by coupling structural dynamics, analysis and thermodynamics calculations. Fin structure was selected for a heater and a cooler to increase heat exchange area and improve heat transfer performance. Size of gap used for clearance seal was designed and completed by precision machining processing, which was a key step of the whole engine manufacturing (Jia *et al.*, 2012). The designed free-piston Stirling engine worked at a relatively low differential temperature. The free piston Stirling engine was a beta-type configuration. The free piston Stirling engine was coupled with a pneumatic cylinder and results by simulation showed that the output power from numerical simulation was higher than that of the experiment according to theoretical assumptions (Kwankaomeng & Promvong, 2010). Gamma type Stirling engine was designed and developed for application of waste heat recovery system. The performance of low temperature difference Stirling engine was investigated. A twin power piston, gamma configuration, low temperature differential Stirling engine was tested with non-pressurized air by using a solar simulator and conclusions were that the Stirling engine working with relatively low air temperature would be a potentially attractive future engine (Dadi *et al.*, 2012).

2.3.3 Waste Heat for Refrigeration Purposes

Heat recovery from automotive engines has been predominantly used for turbo-charging or for cabin heating with application of absorption chillers. Experiments conducted on the system, prove that the concept is feasible, and could significantly enhance system performance depending on part-load of the engine. Also the concept could be used for refrigeration and air conditioning of transportation vehicles (Talom & Beyene, 2009). A systematic view of vapour absorption cycle is shown in Figure 2.5. A novel adsorption air-conditioning system used in internal combustion engine for a cooling locomotive driver cabin was investigated. This system employs zeolite-water as working pairs and is driven by the waste heat from exhaust gas of internal combustion engine. The refrigeration capacity can be provided continuously and steadily to the locomotive driver cabin for space cooling instead of the electric vapour compression air-conditioning system. Experiments showed that single absorber with regenerator locomotive driver cabin air-conditioning system is simple in structure, reliable in operation, and convenient to control (Jiangzhou *et al.*, 2003). An absorption refrigeration unit interfaced with a Caterpillar diesel engine has been used for cooling the charge air prior to ingestion to the engine cylinder or for other cooling purposes such as air conditioning. Research has shown that a diesel absorption combined cycle with pre-inter cooling will have a higher power output and a thermal efficiency than the other configurations. On the other hand the overall efficiency of a pre inter cooled cycle is lower than that of the inter-cooler (Talbi & Agnew, 2002).

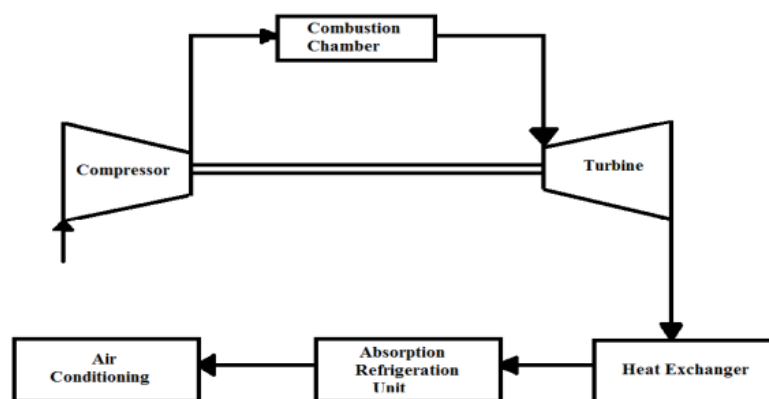


Figure 2. 5: Vapour absorption cycle

(Source: Jadhao & Thombare, 2013)

2.3.4 Waste Heat for Mechanical Turbo-compounding Purposes

A turbo-compound engine is an internal combustion engine that has a power turbine to recover energy from the exhaust gases. The turbine could either be mechanically coupled to a gear and crankshaft that can provide additional power to the engine or be connected to a generator and produces electricity, which can power on board auxiliaries or stored in a battery. The most dominating technologies for exhaust energy recovery are thermoelectric generators to convert heat directly to electricity, implementation of Rankine cycle through an expander, Stirling engine, mechanical turbo compounding and electrical turbo compounding (Hountalas *et al.*, 2007). Studies show that mechanical turbo compounding can reduce the brake specific fuel consumption (BSFC) by 5.7%. However, this value depends strongly on the efficiency of the power-turbine. By adding a power-turbine in the exhaust flow, up to 20% of exhaust energy recovery is possible which equals to about 5% of total fuel energy (Greszler, 2008). Besides that, engine peak power output can also be increased by up to 10% and overall thermal efficiency improvement by 3-5%. A compressor and turbine on a single shaft is used to boost the inlet air (or mixture) density. Energy available in the engine's exhaust gas is used to drive a turbine which drives the turbocharger compressor raising the inlet fluid density prior to entry to each engine cylinder. A turbocharged and turbo-compounded internal combustion engine is shown in Figure 2.6. The turbo demonstrates a method that is presently utilized widely to convert waste energy to improve the efficiency and power output of the internal combustion engine. The problem with current turbochargers is that they do not extract all the possible energy available. The concept of using a turbine to recover energy comes from the turbocharger. The turbocharger is a mechanism that increases the power output of the engine using a turbine. Rather than using the turbine to power a compressor, the turbine could be connected to a generator. Alternatively, a series of turbines could be connected to a series of generators. If an efficient design was implemented the alternator could be removed from the car to improve the efficiency of the engine by lowering the load on it and by decreasing the weight of the car itself. A turbine of this nature would have to be situated after the catalytic converter (Pandiyarajan *et al.*, 2011). Indeed turbo compounding does give improvements however, there are many other exhaust energy recovery method that has proven to give more improvement such as the Rankine cycle (Mavropoulos & Hountalas, 2010; Weerasinghe *et al.*, 2010), although turbo compounding has its own benefits and advantages mainly in its attractive cost and wide applicability.

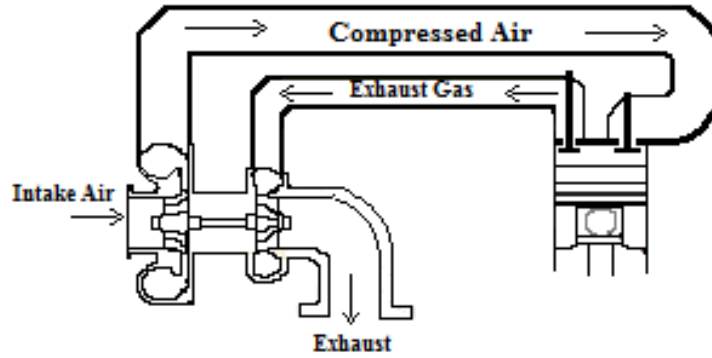


Figure 2. 6: Turbocharger

(Source: Jadhao & Thombare, 2013)

2.4 Waste Heat Recovery Benefits

Recovery of waste heat has a direct effect on the combustion process efficiency. This is reflected by reduction in the utility consumption and process cost. Indirect benefits include; reduction in pollution: A number of toxic combustible wastes such as carbon monoxide (CO), hydrocarbons (HC), nitrogen oxides (NO_x), and particulate matter (PM) are usually released to the atmosphere. Recovering of heat reduces the environmental pollution levels. Reduction in equipment sizes: Waste heat recovery reduces the fuel consumption, which leads to reduction in the flue gas produced. This results in reduction in equipment sizes. Reduction in auxiliary energy consumption: Reduction in equipment sizes gives additional benefits in the form of reduction in auxiliary energy consumption (Teng *et al.*, 2007). Among various advanced concepts, exhaust energy recovery for internal combustion (IC) engines has been proved to not just bring measurable advantages for improving fuel consumption but also increase engine power output (power density) or downsizing, further reducing CO₂ and other harmful exhaust emissions correspondingly (Arias *et al.*, 2006). It was predicted that if 6% of the heat contained in the exhaust gases were converted to electric power, 10% reduction of fuel consumption can be achieved (Vázquez *et al.*, 2002).

2.5 Air as a Drying Fluid

Drying of grains ideally provide long time storage without degradation. This helps to reduce post-harvest losses and also improves quality. Air as a drying fluid has several responsibilities, such as: carrying the heat needed for evaporation of the moisture, transport of the evaporated water out of the plant, and, after the drying process is finished, to cool down the dried product (Dincer *et al.*, 2002). Temperature of the warm air has limited values

depending on the products in question. For example, the maximum recommended temperature for drying grains is usually 43°C as revealed by reviewed literature (Karathanos & Belessiotis, 1999) and most of the grains would be damaged if they were submitted to a temperature of 52°C. When grains are milled, temperatures above 60°C are not allowed (Aukah *et al.*, 2015). Consequently, the duration of drying process will depend on the maximum allowed temperature, i.e. the higher the temperature of the drying air, the shorter the time to dry the product. (Krokida & Maroulis, 2000) reported that physical and chemical damaging may occur to the products when higher temperatures than the allowed in drying are experienced. In grains (rice, corn, soybeans) higher temperatures may cause cracking and reduce viability. According to Hashemi *et al.* (2003), higher temperatures than the allowed for fruit and vegetables in question would cause damage of the nutrients, structure, aroma deterioration, loss of the typical color and other quality losses. To avoid such negative consequences, it is necessary: to use lower temperatures for drying, to cool the dried grains slowly, to remove only a limited part of moisture content (different for each type of product) and to use air with certain humidity as drying fluid at elevated temperature (Braun *et al.*, 2002).

2.6 Summary of the Reviewed Literature

The reviewed literature shed light on the operation cycle of a tractor engine and the possibility of exhaust gas heat energy recovery from stationery tractor engines. Imperatively, direct and indirect waste heat recovery methods and utilization were reviewed. Current utilization of exhaust gas heat for power generation, refrigeration, heating and mechanical turbo-compounding purposes were discussed in the literature. Emphasis was made on the importance of transient impact knowledge on waste heat recovery potential from agricultural machines. Energy analyses of exhaust in transient conditions show evidence of unsteady and unpredictable behavior in tractor engines. Previous study suggested that the wasted energy in diesel engines represents about two-thirds of the input energy and the amount of such loss, recoverable at least partly depends on the engine load. The literature on air as a drying fluid and exhaust gas properties helps in understanding the process of moisture removal from agricultural products.

In the light of the above discussion of relevant literature, it is hoped that this research on energy recovery makes contribution to existing knowledge in the wide and ever changing field of engineering. The knowledge gap as found from the reviewed literature is that exhaust gas heat recovery technique would ultimately reduce the use of conventional fossil fuel

energy. Moreover, the literature review also revealed that exhaust gas heat energy has not been used for maize grain drying. In addressing the knowledge gap, this study on exhaust energy recovery seeks to achieve a reduction or elimination of the need for propane gas use in grain drying systems contemporarily used by Kenyan maize growers. The identified knowledge gap may further be addressed in this study through the intended use of the recovered heat energy from a stationary diesel engine exhaust; to simulate maize drying from a moisture content of 25% to 13%.

CHAPTER THREE

MATERIALS AND METHODS

3.1 Experimental Set-up

This research was conducted at Jomo Kenyatta University of Agriculture and Technology, School of Mechanical and Manufacturing Engineering, thermo-fluids laboratory. The experimental set-up as shown in Figure 3.1 consisted of a single cylinder, four-stroke, multi-fuel engine connected to an eddy current dynamometer for loading at various engine speeds for diesel and biodiesel fuels. Experiments were conducted for the two fuels at engine speeds of 1000, 1250 and 1500 rpm and torque loads of 6 to 22 Nm at intervals of 4 Nm in accordance with the manufacturer's recommendations. The dynamometer was bidirectional. The shaft mounted finger type rotor ran in a dry gap. A closed circuit type cooling system permitted for a sump. Dynamometer load measurement was from a strain gauge load cell and speed measurement was from a shaft mounted three hundred sixty pulses per revolution rotary encoder. To control the speed, a set speed was given to the controller. If the measured speed of the shaft was less than that of the set speed, the load was decreased and vice versa. Since the engine had sufficient torque to attain the set speed, this maintained a constant speed. To control the load, a set load was given to the controller. If the measured load on the dynamometer was greater than that of the set load, the load was decreased and the reverse was also done if the measured load was less. Since the engine had sufficient torque to attain the set load, this maintained a constant load while the speed varied.

3.2 Data Collection

The setup enabled the measurement and collection of the following data: fuel consumption (kg/hr); air consumption (kg/hr); brake power (kW); exhaust gas to calorimeter inlet temperature (°C); and exhaust gas from calorimeter outlet temperature (°C). The instrumentation of the engine was mainly equipped with a data acquisition system and ICE Software. Data was collected using LabView 9.0. LabView based software (Enginesoft) was used for engine performance analysis and evaluation. Data was displayed on a windows based personal computer screen in real time basis and the results were simultaneously recorded in Excel file format.

Table 3. 1: Parts of research engine test setup

Research Engine Test Setup Components		
1. Test Bench Bed	2. Hydraulic Pressure Gauge	3. Control Signal Input Lines
4. Torque Signal Lines	5. Dynamometer	6. Temperature Sensor
7. Water Level Sensor	8. Exhaust Temperature Sensor	9. Exhaust Pipe
10. Oil Temperature Signal Lines		11. Cooling Fan Dome
12. Engine		13. Fuel Flow Signal Lines
14. Fuel Consumption Instrument		15. Pipeline
16. Air Filter		17. Coupling
18. Speed Sensor		19. FC 2000 Control Box
20. Connecting Wire		

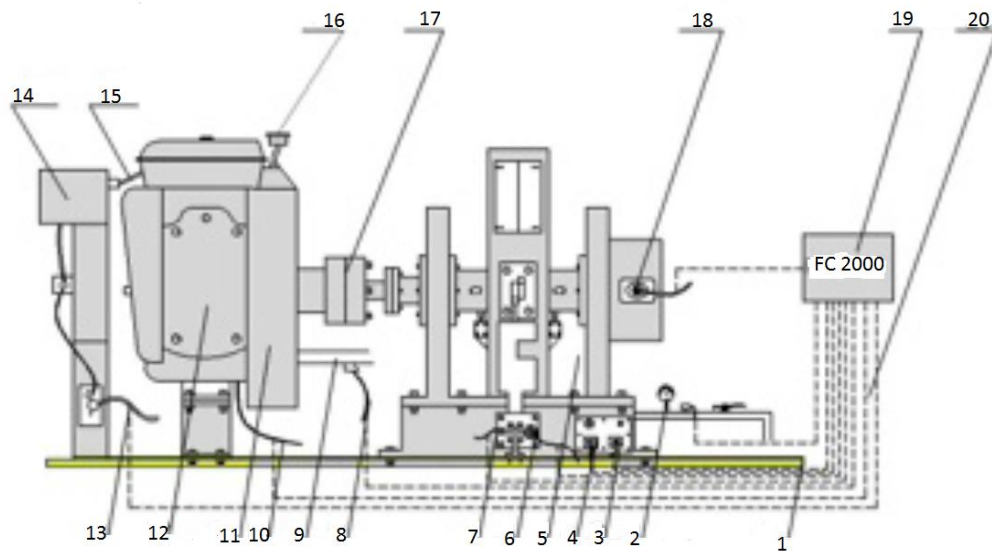


Figure 3. 1: Research engine test setup

3.3 Fuel Energy

Calorific values of the two fuels: diesel and biodiesel were used as 42000kJ/kg and 37800kJ/kg respectively as recommended by American society for testing and materials (ASTM) international D1826-94(1998). *Codiaeum variegatum* (Croton) nut biodiesel was

used in this study. From Equation 3.1 fuel energy was a product of fuel consumption data and calorific value for the two fuels when the engine was operated at different speeds and torque loads.

$$\dot{Q}_F = \dot{m}_f \times CV \quad (3.1)$$

Where:

$$\dot{Q}_F = \text{Fuel energy (kJ/h)}$$

$$\dot{m}_f = \text{Fuel consumption (kg/h)}$$

$$CV = \text{Calorific value (kJ/kg)}$$

3.4 Heat Lost through Exhaust

From the data collected, recorded values of air and fuel consumption; and exhaust gas to calorimeter inlet temperature were used in calculations. The specific heat capacity of exhaust gas was taken as 1.006 kJ/kg°C. The ambient temperature was recorded as 24 °C. The quantity of heat lost in the exhaust gas was determined as given in Equation 3.2.

$$\dot{Q}_L = (\dot{m}_a + \dot{m}_f) \times C_p \times (T_i - T_a) \quad (3.2)$$

Where:

$$\dot{Q}_L = \text{Energy lost in exhaust gas (kJ/h)}$$

$$\dot{m}_a = \text{Air consumption (kg/h)}$$

$$\dot{m}_f = \text{Fuel consumption (kg/h)}$$

$$C_p = \text{Specific heat capacity of exhaust gas (kJ/kg°C)}$$

$$T_i = \text{Exhaust gas to calorimeter inlet temperature (°C)}$$

$$T_a = \text{Ambient temperature (°C)}$$

3.5 Heat Energy Recovered

A pipe calorimeter with a volume of 0.06 m³ was used to determine the changes in exhaust gases energy. Thermocouple temperature sensors and transmitters were used for temperature measurement. Data was obtained for: air and fuel consumption; exhaust gas to calorimeter inlet temperature; and exhaust gas from calorimeter outlet temperature. The specific heat capacity of exhaust gas was used as 1.006 kJ/kg°C. The quantity of energy recovered in the exhaust gas was determined as given in Equation 3.3.

$$\dot{Q}_R = (\dot{m}_a + \dot{m}_f) \times C_p \times (T_i - T_o) \quad (3.3)$$

Where:

\dot{Q}_R = Energy recovered from exhaust gas (kJ/h)

\dot{m}_a = Air consumption (kg/h)

\dot{m}_f = Fuel consumption (kg/h)

C_p = Specific heat capacity of exhaust gas (kJ/kg°C)

T_i = Exhaust gas to calorimeter inlet temperature (°C)

T_o = Exhaust gas from calorimeter outlet temperature (°C)

3.6 Grain Drying Models

For purposes of estimating the amount of maize that could be dried with the recovered energy, safe and recommended temperatures were used. The dryer had a rated capacity of 1900 kg/h. Drying air forced by a fan past a propane burner entered the air plenum through the grain chamber to dry the grain at an inlet temperature of 45°C. The drying air exited the dryer at an outlet temperature of 25°C with a relative humidity (ϕ) of 78%. These conditions were used in a psychrometric chart to determine other air properties. The aim of the research was to simulate maize drying from initial moisture content (m_i) of 25% wb to a final moisture content (m_f) of 13% wb. Initial moisture (M_i) and final moisture content (M_f) on dry basis were determined from Equation 3.4 and Equation 3.5.

$$M_i(db) = \frac{m_i(wb)}{1 - m_f(wb)} \quad (3.4)$$

$$M_f(db) = \frac{m_f(wb)}{1 - m_f(wb)} \quad (3.5)$$

Determination of mass balances for dry matter and water were done using Equation 3.6, Equation 3.7, Equation 3.8 and Equation 3.9.

$$\dot{m}_{wi} = \text{Rated capacity} \times m_i(wb) \quad (3.6)$$

$$\dot{m}_{dmi} = \dot{m}_{dmf} = \text{Rated capacity} - \dot{m}_{wi} \quad (3.7)$$

$$\dot{m}_{wvf} = \dot{m}_{dmf} \times M_f(db) \quad (3.8)$$

$$\Delta \dot{m}_w = \dot{m}_{wi} - \dot{m}_{wvf} \quad (3.9)$$

Where:

\dot{m}_{wi} = Initial mass flow rate of water (kgH₂O/h)

\dot{m}_{wf} = Final mass flow rate of water (kgH₂O/h)

\dot{m}_{dmi} = Initial mass flow rate of dry matter (kgdm/h)

\dot{m}_{dmf} = Final mass flow rate of dry matter (kgdm/h)

$\Delta\dot{m}_w$ = Change in mass flow rate of water (kgH₂O/h)

Moisture gained by each unit mass of dry air was determined from Equation 3.10.

$$\Delta\omega = \omega_f - \omega_i \quad (3.10)$$

Where:

$\Delta\omega$ = Change in each unit mass of dry air (kgH₂O/kgDA)

ω_f = Final unit mass of dry air (kgH₂O/kgDA)

ω_i = Initial unit mass of dry air (kgH₂O/kgDA)

Mass flow rate of dry air was determined from Equation 3.11 and energy required to dry 1 kg of maize was determined from Equation 3.12. The amount of maize (kg/h) that could be dried with the recovered energy from the exhaust gases was determined from Equation 3.13.

$$\dot{m}_{DA} = \frac{\Delta\dot{m}_w}{\Delta\omega} \quad (3.11)$$

$$\dot{Q}_r = \frac{h \times \dot{m}_{DA}}{\text{Rated capacity}} \quad (3.12)$$

$$\text{Grain dried} = \frac{\dot{Q}_R}{\dot{Q}_r} \quad (3.13)$$

Where:

\dot{m}_{DA} = Mass flow rate of dry air (kgDA/h)

$\Delta\dot{m}_w$ = Change in mass flow rate of water (kgH₂O/h)

$\Delta\omega$ = Change in each unit mass of dry air (kgH₂O/kgDA)

h = Enthalpy at saturation (kJ/kgDA)

\dot{Q}_R = Energy recovered from exhaust gas (kJ/h)

\dot{Q}_r = Specific energy required to dry maize (kJ/kg)

CHAPTER FOUR

RESULTS AND DISCUSSIONS

4.1 Thermal Energy Lost through Exhaust

As discussed in the methodology, this study used a 3.5 kW single cylinder, four-stroke, multi-fuel engine which was operated on diesel and biodiesel fuels. Diesel fuel had a calorific value of 42000kJ/kg and croton nut biodiesel had a calorific value of 37800kJ/kg. The engine was operated at three different speeds of 1000 rpm, 1250 rpm, and 1500 rpm. At each speed an eddy current dynamometer was used to load the engine at 6 Nm, 10 Nm, 14 Nm, 18 Nm, and 22 Nm. Table 4.1 and Table 4.2 presents results of: fuel energy for different engine speeds and torque loads and heat energy lost through exhaust for diesel and biodiesel fuels.

In the case of diesel fuel, when the engine was operated at 1000 rpm and loaded at 6 Nm, the heat energy entering the exhaust was 2% of the fuel energy. When the load was increased to 10 Nm, the heat energy entering the exhaust was 2.5% of the fuel energy. At 14 Nm the heat energy entering the exhaust was 5.2% of the fuel energy. The heat energy entering the exhaust at 1000 rpm for diesel fuel at a load of 18 Nm was 7.1% of the fuel energy. Loading the engine at 22 Nm showed that the heat energy entering the exhaust was 7% of the fuel energy. It can be concluded that torque loads between 6 Nm to 18 Nm had an increasing effect on the heat energy entering the exhaust since the corresponding results of percentages of the fuel energy were found as: 2%, 2.5%, 5.2% and 7.1%. Figure 4.1 illustrates the variations of the heat energy entering the exhaust versus torque loads at an engine speed of 1000 rpm. In the case of biodiesel fuel, when the engine was operated at 1000 rpm and loaded at 6 Nm, the heat energy entering the exhaust was 1.6% of the fuel energy. When the load was increased to 10 Nm, the heat energy entering the exhaust was 2.6% of the fuel energy. At 14 Nm the heat energy entering the exhaust was 5.6% of the fuel energy. Heat energy entering the exhaust at 1000 rpm for biodiesel fuel at a load of 18 Nm was 7.7% of the fuel energy. Loading the engine at 22 Nm showed that the heat energy entering the exhaust was 7.3% of the fuel energy. Torque loads of 6 Nm to 18 Nm had an increasing effect on heat energy entering the exhaust since the percentages of the fuel energy corresponding to them were: 1.6%, 2.6%, 5.6% and 7.7%.

Table 4. 1: Fuel energy (kJ/h) for different engine speeds and torque loads

Fuel	Speed	Torque Loads				
		6 Nm	10 Nm	14 Nm	18 Nm	22 Nm
Diesel	1000rpm	50295 ±11739	57435 ±7018	46305 ±11050	51870 ±5796	56280 ±8648
	1250rpm	84945 ±8887	76020 ±8748	80010 ±7263	68985 ±13245	78225 ±9320
	1500rpm	64680 ±25256	63315 ±22619	69720 ±20261	68040 ±17510	64890 ±19948
Biodiesel	1000rpm	61520 ±2485	59252 ±2762	53109 ±4626	54621 ±6833	55472 ±3571
	1250rpm	79475 ±1614	73805 ±1418	75222 ±772	73332 ±2041	74750 ±1418
	1500rpm	18900 ±0	25043 ±905	30240 ±1336	35438 ±1189	46683 ±11567

Table 4. 2: Heat energy (kJ/h) lost through exhaust for different engine speeds and torque loads

Fuel	Speed	Torque Loads				
		6 Nm	10 Nm	14 Nm	18 Nm	22 Nm
Diesel	1000rpm	984 ±95	1419 ±219	2416 ±433	3711 ±539	3938 ±863
	1250rpm	1925 ±202	2052 ±251	2545 ±369	3787 ±252	4818 ±811
	1500rpm	2861 ±158	3364 ±162	4644 ±444	4919 ±565	4824 ±753
Biodiesel	1000rpm	985 ±100	1541 ±169	2971 ±164	4219 ±287	4061 ±690
	1250rpm	2100 ±115	2352 ±331	3738 ±316	5058 ±164	5797 ±106
	1500rpm	3435 ±76	4155 ±323	5680 ±343	5955 ±28	5889 ±79

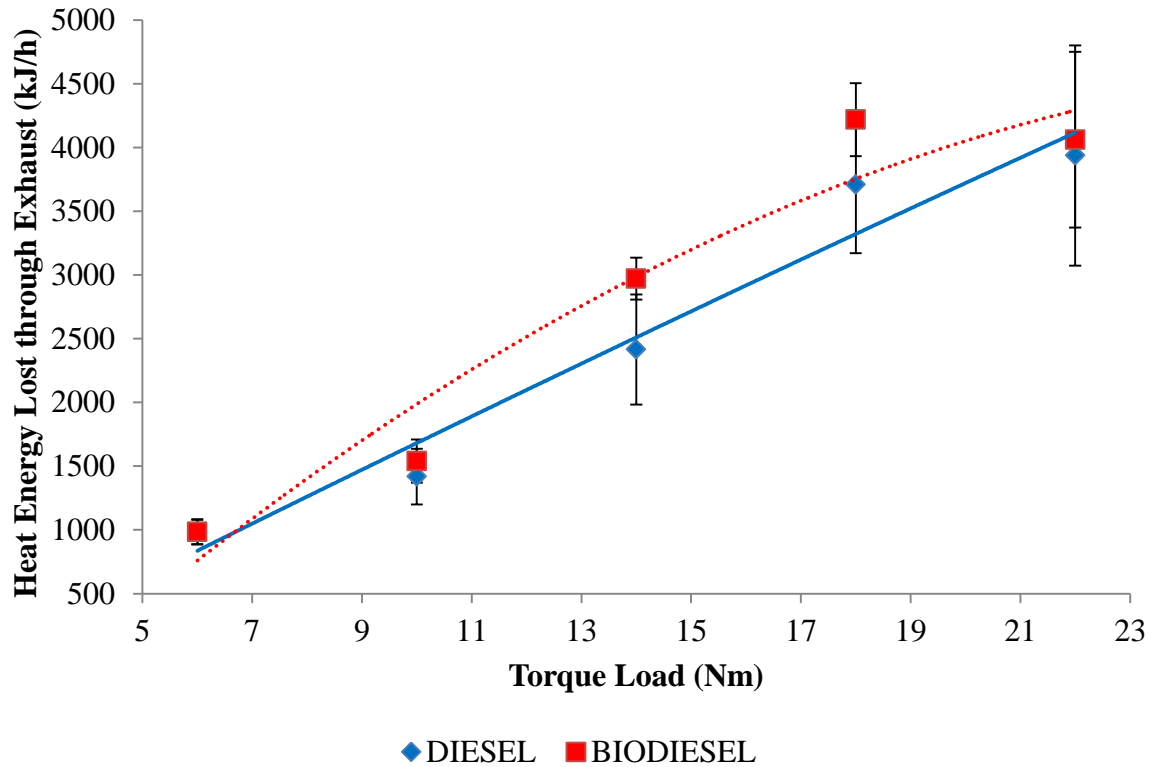


Figure 4. 1: Heat energy lost through exhaust against torque load at 1000 rpm

Punov *et al.* (2013) evaluated the energy and exergy available at different location points in the exhaust system of a tractor engine and from the energy balance of the engine, found that more than 35% of the fuel energy is lost by exhaust gases on the most typical operating points. Increasing the engine speed to 1250 rpm and loading at 6 Nm, in the case of diesel fuel, showed that the heat energy entering the exhaust was 2.3% of the fuel energy. When the load was increased to 10 Nm, the heat energy entering the exhaust was 2.7% of the fuel energy. At 14 Nm the heat energy entering the exhaust was 3.3% of the fuel energy. The heat energy entering the exhaust at 1250 rpm for biodiesel fuel at a load of 18 Nm was 5.5% of the fuel energy. Loading the engine at 22 Nm increased the heat energy entering the exhaust to 6.2% of the fuel energy. Torque load had an increasing effect on the heat energy entering the exhaust since the percentages of the fuel energy were found to be: 2.3%, 2.7%, 3.3%, 5.5% and 6.2% corresponding to the increased loading at intervals of 4 Nm from 6 Nm to 22 Nm.

For biodiesel fuel, when the engine was operated at 1250 rpm and loaded at 6 Nm, the heat energy entering the exhaust was 2.6% of the fuel energy. When the load was increased to 10 Nm, the heat energy entering the exhaust was 3.2% of the fuel energy. At 14 Nm the heat

energy entering the exhaust was 4.9% of the fuel energy. The heat energy entering the exhaust at 1250 rpm for biodiesel fuel at a load of 18 Nm was 6.9% of the fuel energy. Loading the engine at 22 Nm increased the heat energy entering the exhaust to 7.7% of the fuel energy. Figure 4.2 illustrates the variations of the heat energy entering the exhaust versus torque loads at an engine speed of 1250 rpm. For this speed, it can be concluded that torque load had an increasing effect on the heat energy entering the exhaust since the percentages of the fuel energy increased from 2.6% to 7.7%.

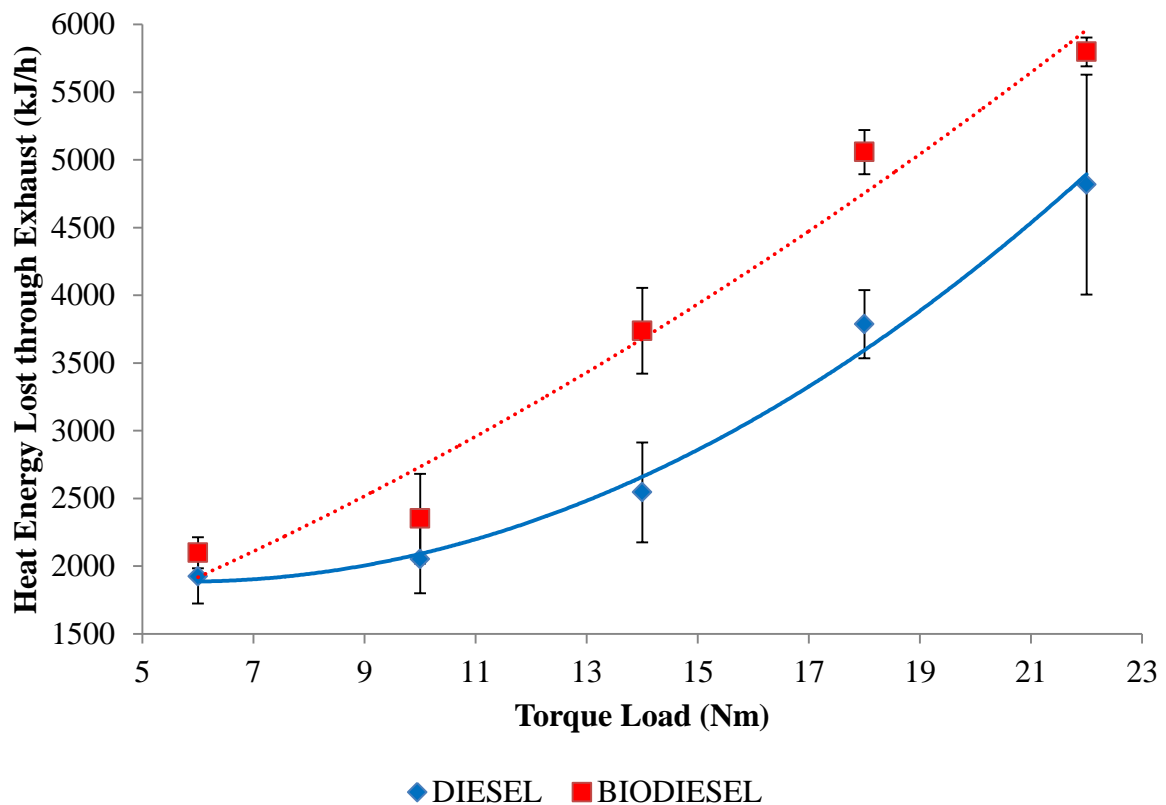


Figure 4. 2: Heat energy lost through exhaust against torque load at 1250 rpm

In this study, the highest engine speed used was 1500 rpm. For diesel fuel, at the lowest load of 6 Nm, the heat energy entering the exhaust was 4.4% of the fuel energy. The heat energy entering the exhaust at 1500 rpm for diesel fuel at a load of 10 Nm was 5.3% of the fuel energy. At 14 Nm the heat energy entering the exhaust was 6.7% of the fuel energy. The heat energy entering the exhaust at 1500 rpm for diesel fuel at a load of 18 Nm was 7.2% of the fuel energy. Loading the engine at 22 Nm reduced the heat energy entering the exhaust to 7.4% of the fuel energy. Torque load had an increasing effect on the heat energy entering the exhaust since the percentages of the fuel energy were found to be: 4.4%, 5.3%, 6.7%,

7.2% and 7.4% corresponding to the increased loading at intervals of 4 Nm from 6 Nm to 22 Nm.

In the case of biodiesel fuel, the heat energy entering the exhaust at 1500 rpm for at a load of 6 Nm was 18.2% of the fuel energy. When the load was increased to 10 Nm, the heat energy entering the exhaust was 16.6% of the fuel energy. A load of 14 Nm reduced the heat energy entering the exhaust to 18.7% of the fuel energy. The heat energy entering the exhaust at 1500 rpm for biodiesel fuel at a load of 18 Nm was 16.8% of the fuel energy. Loading the engine at 22 Nm reduced the heat energy entering the exhaust to 12.6% of the fuel energy. Figure 4.3 illustrates the variations of the heat energy entering the exhaust versus torque loads at an engine speed of 1500 rpm.

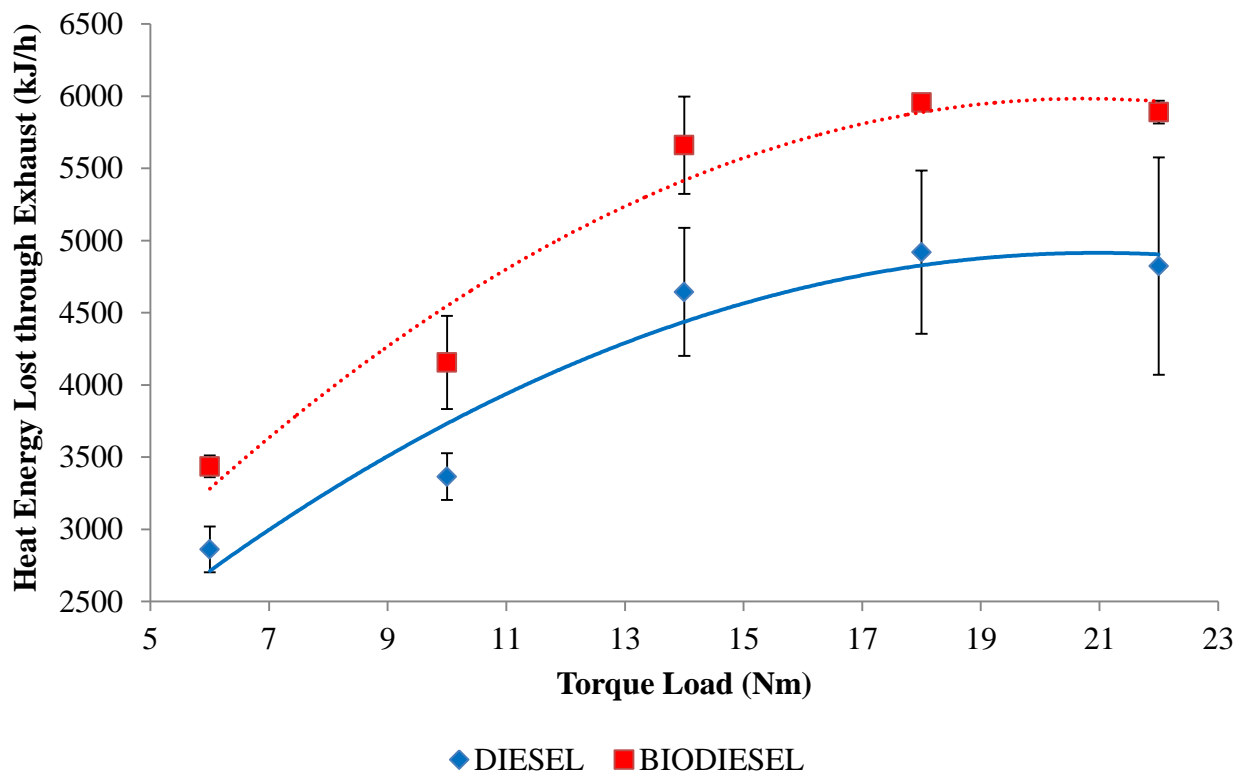


Figure 4. 3: Heat lost through exhaust against torque load at 1500 rpm

Studies have shown that the energy lost in exhaust gases increases substantially with increased exhaust gas temperature (Canakci, 2005; Hansen & Jensen, 1997; Rahman *et al.*, 2013). In this study, temperature ranges of exhaust gas from engine were between 220°C to 330°C. Nadaf and Gangavati (2014) reported 315°C to 600°C as the temperature range of exhaust gases from a non turbo charged reciprocating engine; turbo charged engines had a

temperature range of 230°C to 370°C. Table 4.3 presents the observed readings of exhaust gas to calorimeter inlet temperature for different engine speeds and torque loads.

Table 4. 3: Exhaust gas to calorimeter average inlet temperature (°C) for different engine speeds and torque loads

Fuel	Speed	Torque Load				
		6 Nm	10 Nm	14 Nm	18 Nm	22 Nm
Diesel	1000 rpm	227	235	265	302	318
	1250 rpm	252	266	283	312	324
	1500 rpm	286	314	321	317	310
Biodiesel	1000 rpm	221	230	265	306	324
	1250 rpm	245	257	288	319	331
	1500 rpm	298	327	331	324	318

The results for exhaust gas to calorimeter inlet temperature when the engine was operated on diesel fuel at a speed of 1000 rpm show that exhaust gas to calorimeter inlet temperature was 2.76% higher than when the engine used biodiesel at a torque load of 6 Nm. When the torque load was increased to 10 Nm, exhaust gas to calorimeter inlet temperature for diesel fuel was 2.38% higher than biodiesel fuel. While maintaining the engine speed at 1000 rpm and increasing the torque load at an interval of 4 Nm to 14 Nm, the exhaust gas to calorimeter inlet temperature corresponding to this load for diesel fuel was 0.03% higher than biodiesel fuel. At a torque load of 18 Nm, exhaust gas to calorimeter inlet temperature for diesel fuel was 1.3% lower than biodiesel fuel. When the torque load was increased to 22 Nm, exhaust gas to calorimeter inlet temperature result was 1.87% lower when the engine was operated on diesel in comparison to biodiesel.

Increasing the engine speed to 1250 rpm gave the results of exhaust gas to calorimeter inlet temperature as 2.75% higher when diesel fuel was used as compared to biodiesel at a torque load of 6 Nm. Moreover, exhaust gas to calorimeter inlet temperature for diesel fuel was 3.28% higher than biodiesel at a torque load of 10 Nm. Similarly, at the engine speed of 1250 rpm and a torque load of 14 Nm, exhaust gas to calorimeter inlet temperature for diesel fuel was 1.72% lower than biodiesel. However, when the torque load was increased to 18 Nm, exhaust gas to calorimeter inlet temperature was 2.29% lower and at 22 Nm, exhaust gas to calorimeter inlet temperature was 1.04% lower when the engine used diesel in comparison to biodiesel.

When the engine was operated at a speed of 1500 rpm with a torque load of 6 Nm, exhaust gas to calorimeter inlet temperature for diesel fuel was 4.07% lower than biodiesel. Subsequently, at a torque load of 10 Nm, exhaust gas to calorimeter inlet temperature for diesel fuel was 4.17% lower than biodiesel. Similarly, at a torque load of 14 Nm, exhaust gas to calorimeter inlet temperature was 2.58% lower when the engine used diesel as compared to biodiesel. Loading the engine at 18 Nm showed that exhaust gas to calorimeter inlet temperature for diesel fuel was 2.08% lower than biodiesel. Finally, at a torque load of 22 Nm, exhaust gas to calorimeter inlet temperature was 2.88% lower when the engine used diesel in comparison to biodiesel.

4.2 Heat Energy Recovered

Table 4.4 shows the results of recovered energy for diesel and biodiesel at different engine speeds and torque loads.

Table 4. 4: Recovered heat energy (kJ/h) for different engine speeds and torque loads

Fuel	Speed	Torque Loads				
		6 Nm	10 Nm	14 Nm	18 Nm	22 Nm
Diesel	1000rpm	224 ± 35	319 ± 74	561 ± 117	636 ± 55	479 ± 127
	1250rpm	308 ± 76	371 ± 81	418 ± 81	482 ± 101	328 ± 141
	1500rpm	508 ± 70	608 ± 77	327 ± 77		
Biodiesel	1000rpm	200 ± 31	322 ± 43	686 ± 43	842 ± 52	652 ± 144
	1250rpm	404 ± 86	425 ± 99	681 ± 99	719 ± 45	339 ± 78
	1500rpm	662 ± 57	650 ± 49	358 ± 104		

In the case of diesel fuel, when the engine was operated at 1000 rpm and loaded at 6 Nm, the recovered energy was 0.445% of the fuel energy and 22.6% of heat energy entering the exhaust. This compares well with a study by Rubaiyat and Bari (2010) where 18% of heat energy entering the exhaust was recovered using a diesel engine. When the load was increased to 10 Nm, the recovered energy was 0.541% of the fuel energy and 22% of heat energy entering the exhaust. At 14 Nm the recovered energy was 1.203% of the fuel energy and 23.3% of heat energy entering the exhaust. The energy recovered at 1000 rpm for diesel fuel at a load of 18 Nm was 1.257% of the fuel energy and 17.8% of heat energy entering the exhaust. Loading the engine at 22 Nm showed that the recovered energy was 0.899% of the fuel energy and 12.8% of heat energy entering the exhaust. It can be concluded that torque loads between 6 Nm to 14 Nm had the same effect on the recovered energy since they gave

percentages of heat energy entering the exhaust as: 22.6%, 22%, and 23.3%. In this study, the maximum recovered energy for the lowest engine speed of 1000 rpm at a load of 18 Nm was 60% of the brake power while in a study by Rubaiyat and Bari (2010) the maximum recovered energy for the lowest engine speed of 1400 rpm was approximately 52% of the brake power when the engine was fueled on diesel. Wei *et al.* (2011) designed a medium temperature waste heat recovery system based on organic Rankine cycle to recover exhaust energy from a heavy duty diesel engine and achieved the highest exhaust waste heat recovery efficiency of 10% to 15% for the optimized heat exchanger design.

In the case of biodiesel fuel, when the engine was operated at 1000 rpm and loaded at 6 Nm, the recovered energy was 0.319% of the fuel energy and 20.024% of heat energy entering the exhaust. When the load was increased to 10 Nm, the recovered energy was 0.538% of the fuel energy and 20.753% of heat energy entering the exhaust. At 14 Nm the recovered energy was 1.285% of the fuel energy and 23.004% of heat energy entering the exhaust. Energy recovered at 1000 rpm for biodiesel fuel at a load of 18 Nm was 1.542% of the fuel energy and 20.029% of heat energy entering the exhaust. Loading the engine at 22 Nm showed that the recovered energy was 1.153% of the fuel energy and 15.688% of heat energy entering the exhaust.

Torque loads of 6 Nm, 10 Nm, 14 Nm and 18 Nm had the same effect on recovered energy since the percentages of heat energy entering the exhaust corresponding to them were: 20.024%, 20.753%, 23.004% and 20.029%. In a related study, simulation work by Hounsham *et al.* (2008) on energy recovery systems for engines showed that there were significant, potential, fuel economy advantages, between 6% and 31%, and high efficiencies could be achieved at practical operating pressures. Baldia *et al.* (2015) reported an improvement of 27% in recoverable exergy of flow at a heat exchanger outlet when the heat exchanger wall thickness was increased from 0.5 mm to 2.5 mm. In this study, the maximum recovered energy for the lowest engine speed of 1000 rpm at 18 Nm was 78% of the brake power when the engine was fueled on biodiesel. Figure 4.4 illustrates the variations of the recovered energy versus torque loads at an engine speed of 1000 rpm.

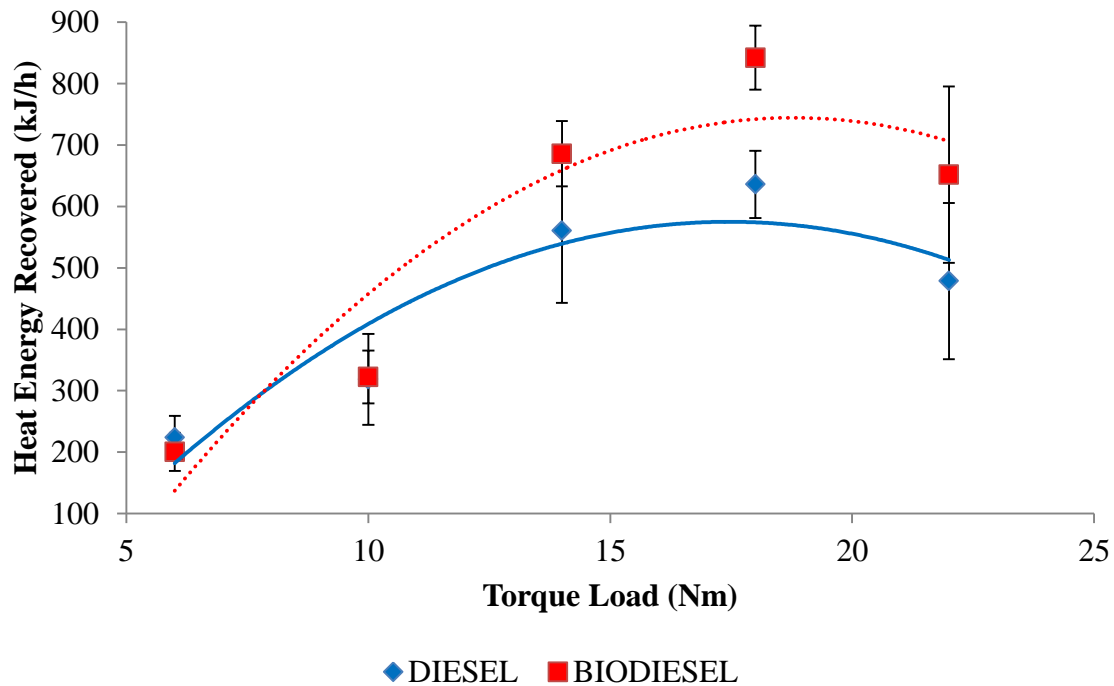


Figure 4. 4: Recovered energy against torque load at 1000 rpm

Increasing the engine speed to 1250 rpm and loading at 6 Nm, in the case of diesel fuel, showed that the recovered energy was 0.349% of the fuel energy and 15.4% of heat energy entering the exhaust. This compares well with a study by Pandiyarajan *et al.* (2011) where a diesel engine integrated with a shell and tube heat exchanger was used to recover 10% to 15% of heat energy entering the exhaust. When the load was increased to 10 Nm, the recovered energy was 0.475% of the fuel energy and 17.5% of heat energy entering the exhaust. At 14 Nm the recovered energy was 0.529% of the fuel energy and 16.2% of heat energy entering the exhaust. The energy recovered at 1250 rpm for biodiesel fuel at a load of 18 Nm was 0.7% of the fuel energy and 12.8% of heat energy entering the exhaust. Loading the engine at 22 Nm reduced the recovered energy to 0.365% of the fuel energy and 5.9% of heat energy entering the exhaust. In this study, the maximum recovered energy for the medium engine speed of 1250 rpm at 18 Nm was 36% of the brake power while in a study by Rubaiyat and Bari (2010) the maximum recovered energy for the medium engine speed of 1800 rpm was approximately 54% of the brake power when the engine was fueled on diesel. In order to improve waste heat recovery, Miller *et al.* (2009) modelled the combination of organic Rankine cycle (ORC) with thermoelectric generator (TEG) in an internal combustion engine (ICE). The authors found that by recovering the high and low temperature waste heat

with the thermoelectric generator and the organic Rankine cycle respectively, the energy recovery capability could be as high as 13.1 kW from a thermal source of 773 K.

For biodiesel fuel, when the engine was operated at 1250 rpm and loaded at 6 Nm, the recovered energy was 0.497% of the fuel energy and 18.8% of heat energy entering the exhaust. When the load was increased to 10 Nm, the recovered energy was 0.555% of the fuel energy and 17.6% of heat energy entering the exhaust. At 14 Nm the recovered energy was 0.903% of the fuel energy and 18.3% of heat energy entering the exhaust. The energy recovered at 1250 rpm for biodiesel fuel at a load of 18 Nm was 0.986% of the fuel energy and 14.3% of heat energy entering the exhaust. Loading the engine at 22 Nm reduced the recovered energy to 0.287% of the fuel energy and 3.7% of heat energy entering the exhaust. In this study, the maximum recovered energy for the medium engine speed of 1250 rpm at 18 Nm was 54% of the brake power when the engine was fueled on biodiesel. Zhang *et al.* (2015) concluded that dual loop organic Rankine cycle while using R123 could generate 32.63 kW. In static gas turbine applications, Larjola (1995) used Toluene as a working fluid to implement an organic Rankine cycle (ORC) system due to its good thermal stability and being less harmful to the environment. Larjola found that as much as 26 kW could be recovered from a 1500 kW gas turbine electric generator. Figure 4.5 illustrates the variations of the recovered energy versus torque loads at an engine speed of 1250 rpm.

In this study, the highest engine speed used was 1500 rpm. For diesel fuel, at the lowest load of 6 Nm, the recovered energy was 0.781% of the fuel energy and 17.66% of heat energy entering the exhaust. The energy recovered at 1500 rpm for diesel fuel at a load of 10 Nm was 0.948% of the fuel energy and 17.74% of heat energy entering the exhaust. At 14 Nm the recovered energy was 0.5% of the fuel energy and 7.49% of heat energy entering the exhaust. Torque loads of 6 Nm and 10 Nm had the same effect on recovered energy since the percentages of the lost exhaust energy corresponding to them were: 17.66% and 17.74%. In this study, the maximum recovered energy for the highest engine speed of 1500 rpm at 10 Nm was 67% of the brake power while in a study by Rubaiyat and Bari (2010) the maximum recovered energy for the highest engine speed of 2200 rpm was approximately 51% of the brake power when the engine was fuelled on diesel. Hossain and Bari (2014) conducted experiments to measure the available exhaust heat from a 40 kW diesel engine generator set and reported 10%, 9% and 8% additional power by using water, ammonia and hydrofluorocarbon-134a as the working fluids respectively.

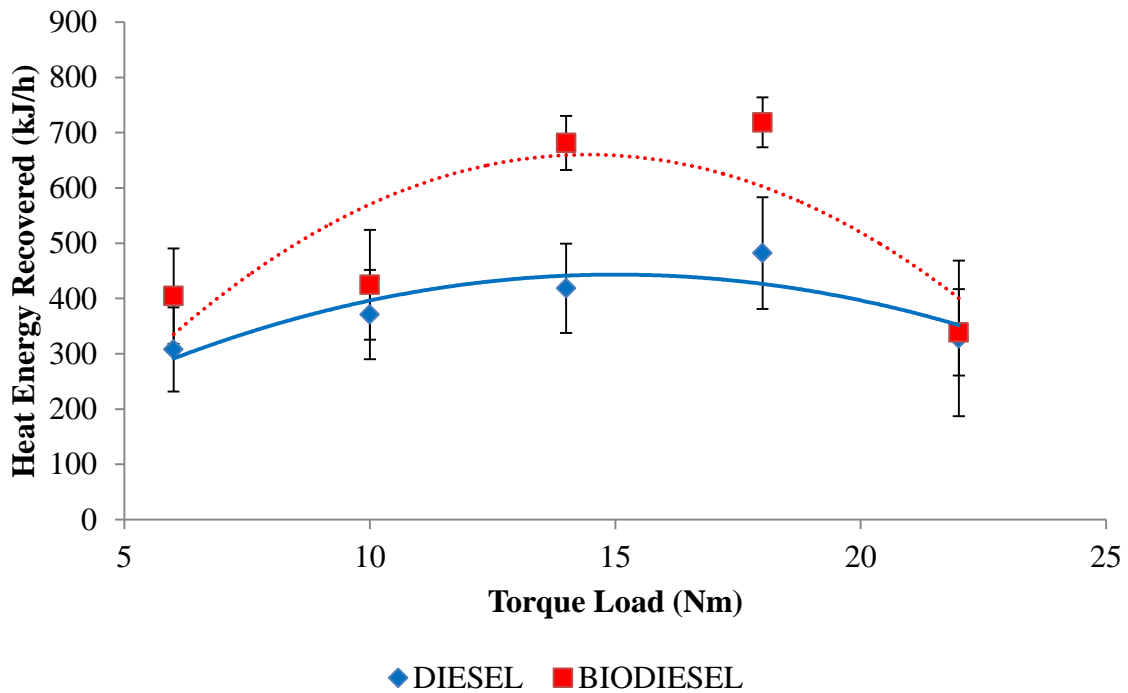


Figure 4. 5: Recovered energy against torque load at 1250 rpm

In the case of biodiesel fuel, the energy recovered at 1500 rpm for at a load of 6 Nm was 3.513% of the fuel energy and 19.3% of heat energy entering the exhaust. When the load was increased to 10 Nm, the recovered energy was 2.626% of the fuel energy and 15.8% of heat energy entering the exhaust. A load of 14 Nm reduced the recovered energy to 1.13% of the fuel energy and 6% of heat energy entering the exhaust. In this study, the maximum recovered energy for the highest engine speed of 1500 rpm at 6 Nm was 23% more as compared to the brake power when the engine was fueled on biodiesel. Figure 4.6 illustrates the variations of the recovered energy versus torque loads at an engine speed of 1500 rpm.

Table 4.5 presents the observed readings of exhaust gas from calorimeter outlet temperature for different engine speeds and torque loads. The results for exhaust gas from calorimeter outlet temperature when the engine was operated on diesel fuel at a speed of 1000 rpm show that exhaust gas from calorimeter outlet temperature was 0.12% lower than when the engine used biodiesel at a torque load of 6 Nm. When the torque load was increased to 10 Nm, exhaust gas from calorimeter outlet temperature for diesel fuel was 0.9% higher than biodiesel. Moreover, when the speed was maintained at 1000 rpm and the torque load increased at intervals of 4 Nm to 14 Nm, exhaust gas from calorimeter outlet temperature for diesel fuel was 0.33% lower than biodiesel. Subsequently, at a torque load of 18 Nm, exhaust

gas from calorimeter outlet temperature corresponding to this load was 1.24% higher when the engine used diesel as compared to biodiesel.

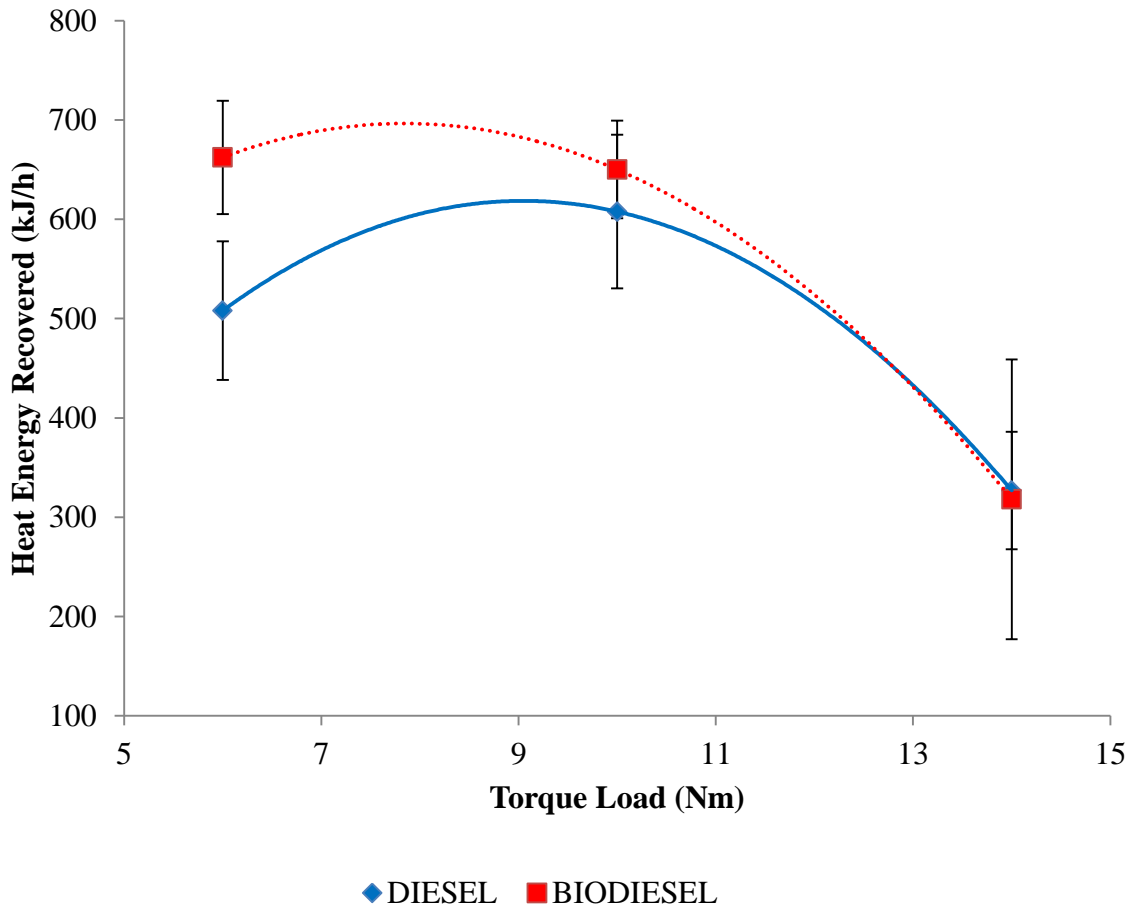


Figure 4. 6: Recovered energy against torque load at 1500 rpm

Table 4. 5: Exhaust gas from calorimeter outlet temperature (°C) for different engine speeds and torque loads

Fuel	Speed	Torque Load				
		6 Nm	10 Nm	14 Nm	18 Nm	22 Nm
Diesel	1000 rpm	181	189	209	252	280
	1250 rpm	217	223	241	275	307
	1500 rpm	240	262	299		
Biodiesel	1000 rpm	181	187	210	249	277
	1250 rpm	203	216	239	277	313
	1500 rpm	245	279	310		

However, at a torque load of 22 Nm, exhaust gas from calorimeter outlet temperature result was 1.26% higher when the engine was operated on diesel in comparison to biodiesel. Increasing the engine speed to 1250 rpm gave the results of exhaust gas from calorimeter outlet temperature as 6.21% higher when diesel fuel was used as compared to biodiesel at a torque load of 6 Nm. Moreover, exhaust gas from calorimeter outlet temperature for diesel fuel was 3.27% higher than biodiesel at a torque load of 10 Nm. Similarly, at the engine speed of 1250 rpm and a torque load of 14 Nm, exhaust gas from calorimeter outlet temperature for diesel fuel was 0.6% higher than biodiesel. However, when the torque load was increased to 18 Nm, exhaust gas from calorimeter outlet temperature was 0.62% lower. At a torque load of 22 Nm, exhaust gas from calorimeter outlet temperature was 3.19% lower when the engine used diesel in comparison to biodiesel.

Comparatively, when the engine was operated at a speed of 1500 rpm with a torque load of 6 Nm, exhaust gas from calorimeter outlet temperature for diesel fuel was 2.09% lower than biodiesel. Subsequently, at a torque load of 10 Nm, exhaust gas from calorimeter outlet temperature for diesel fuel was 6.32% lower than biodiesel. Similarly, at a torque load of 14 Nm, exhaust gas from calorimeter outlet temperature was 4.06% lower when the engine used diesel as compared to biodiesel. Loading the engine at 18 Nm showed that exhaust gas from calorimeter outlet temperature for diesel fuel was 2.22% lower than biodiesel. Finally, at a torque load of 22 Nm, exhaust gas from calorimeter outlet temperature was 0.36% lower when the engine used diesel in comparison to biodiesel.

4.3 Maize Drying Simulation

The specific energy required to dry maize from a moisture content of 25% to 13% wet basis was found to be 1124 kJ/kg. In this study, 750 grams per hour of maize could be dried through simulation at an engine speed of 1000 rpm and a load of 18 Nm when biodiesel was used. In a related study, Basunia *et al.* (1997) used waste heat from an air cooled four-stroke cycle gasoline engine with displacement of 105 cubic centimeters, 1.43 kW at 3000 rpm and 1.85 kW at a maximum speed of 4200 rpm to dry 195 kg of rice in one batch in 14 hours from an initial moisture content of 23% to a final moisture content of 15% on wet basis. Basunia and Abe (2008) found 3150 kJ/kg as the energy requirements to dry 1 kg of rough rice from 23% to 15% moisture content on wet basis.

The result for amount of maize that could be dried with recovered energy when the engine was operated on diesel fuel at a speed of 1000 rpm show that it was 12.2% more than

when the engine used biodiesel at a torque load of 6 Nm. When the torque load was increased to 10 Nm, quantity of maize that could be dried was 2.5% less for the engine fueled with diesel as compared to biodiesel fueling. Moreover, when the speed was maintained at 1000 rpm and the torque load increased from 10 Nm at intervals of 4 Nm to 14 Nm, maize grain to be dried with recovered energy when the engine used diesel fuel was 22.4% less than when biodiesel was used. Subsequently, at a torque load of 18 Nm, 29.1% less could be dried when the engine used diesel as compared to biodiesel. However, at a torque load of 22 Nm, amount of maize grain to be dried resulted in a 26.4% decrease when the engine was operated on diesel in comparison to biodiesel. This is illustrated in Figure 4.7.

As an application, increasing the engine speed to 1250 rpm gave the result of maize grain to be dried with recovered energy as 33.1% less when diesel fuel was used as compared to biodiesel at a torque load of 6 Nm. Moreover, the amount of maize grain that could be dried when the engine used diesel fuel was 13.4% less than when biodiesel was used at a torque load of 10 Nm. Similarly, at the engine speed of 1250 rpm and a torque load of 14 Nm, maize grain that could be dried when the engine used diesel fuel was 60.6% less than when biodiesel was utilized. However, when the torque load was increased to 18 Nm, maize grains to be dried with the recovered energy was 49.7% less and at 22 Nm, quantity of maize grain that could be dried was 24.8% more when the engine used diesel in comparison to biodiesel as presented in Figure 4.8.

Comparatively, when the engine was operated at a speed of 1500 rpm with a torque load of 6 Nm, maize grain that could be dried when the engine used diesel fuel was 31.4% less than when biodiesel was used. Subsequently, at a torque load of 10 Nm, quantity of maize grain that could be dried when the engine used diesel fuel was 9.5% less than when biodiesel was used. Similarly, at a torque load of 14 Nm, maize grains to be dried was 2% more when the engine used diesel as compared to biodiesel as shown in Figure 4.9. In general, maize grain drying potential was found to initially increase from a minimum of 199 g/h to a maximum of 750 g/h with increased engine speed and load for the two fuels. Later it decreased at higher speeds for both fuels at constant loads. For example, at the lowest engine speed of 1000 rpm when the engine was operated on diesel fuel, increased loading from 6 Nm at an interval of 4 Nm to 18 Nm had an increasing effect to a maximum of 566 g/h and later a decreasing effect to 426 g/h with a further load of 22 Nm. A similar trend was observed when the engine was operated on biodiesel. Table 4.6 presents quantity of maize

grain that could be dried with recovered energy from a moisture content of 25% to 13% wet basis.

Table 4. 6: Maize drying potential (g/h) for different engine speeds and torque loads

Fuel	Speed	Torque Loads				
		6 Nm	10 Nm	14 Nm	18 Nm	22 Nm
Diesel	1000rpm	199 ± 31	284 ± 66	499 ± 104	566 ± 49	426 ± 113
	1250rpm	274 ± 68	330 ± 72	373 ± 72	429 ± 90	292 ± 125
	1500rpm	452 ± 62	541 ± 69	291 ± 69		
Biodiesel	1000rpm	178 ± 28	287 ± 38	610 ± 47	750 ± 46	580 ± 128
	1250rpm	360 ± 77	378 ± 88	607 ± 43	640 ± 40	187 ± 153
	1500rpm	590 ± 51	579 ± 44	283 ± 125		

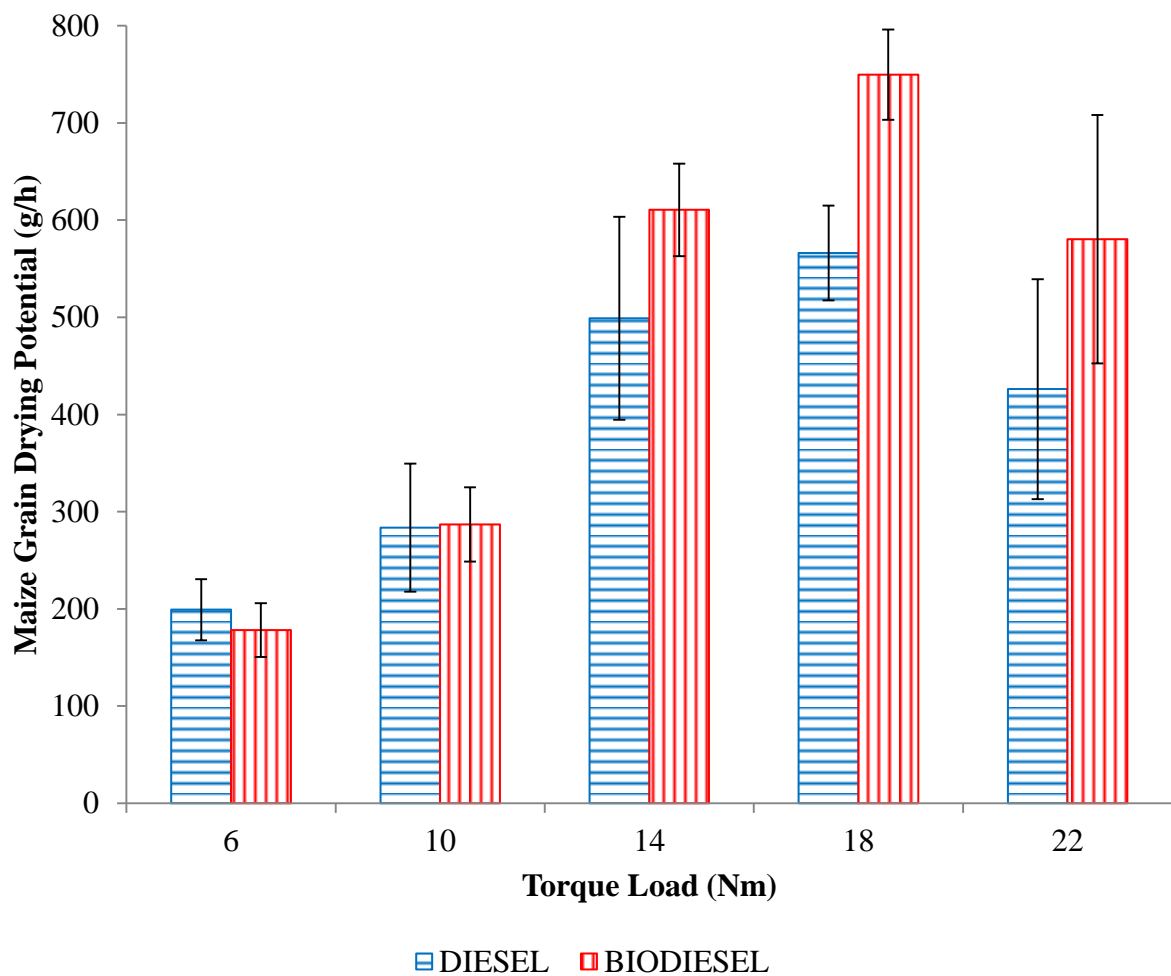


Figure 4. 7: Estimated maize that could be dried against torque load at 1000 rpm

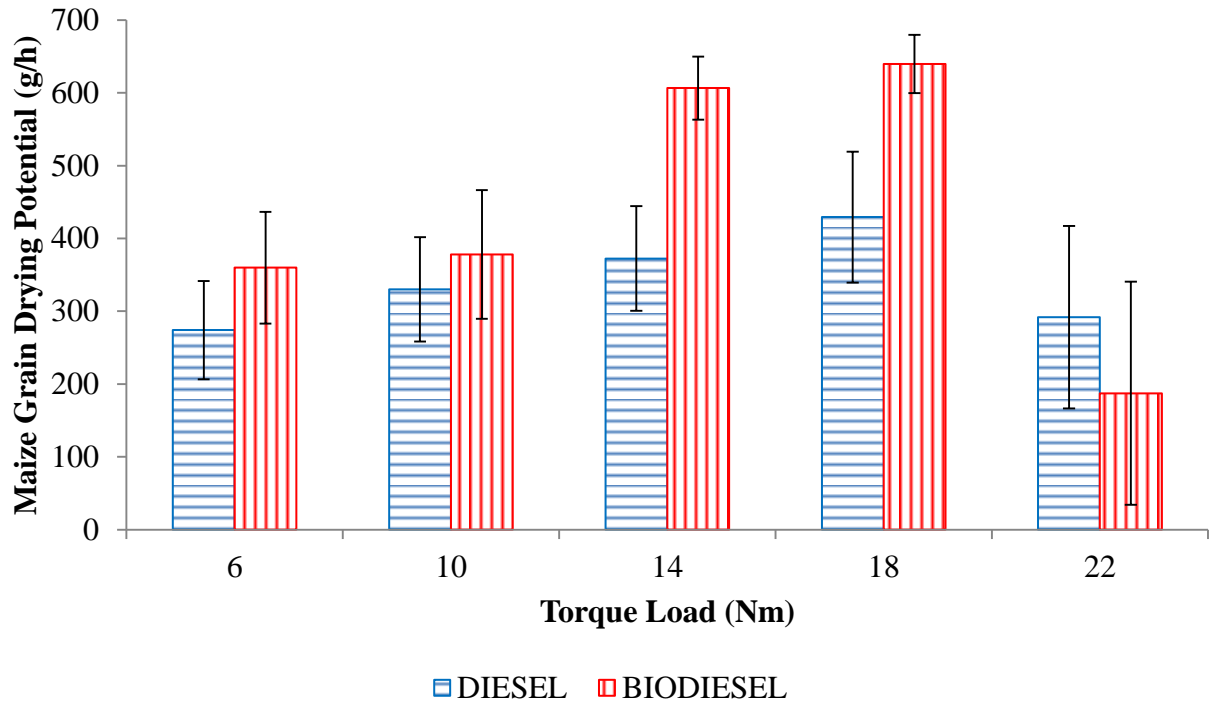


Figure 4. 8: Estimated maize that could be dried against torque load at 1250 rpm

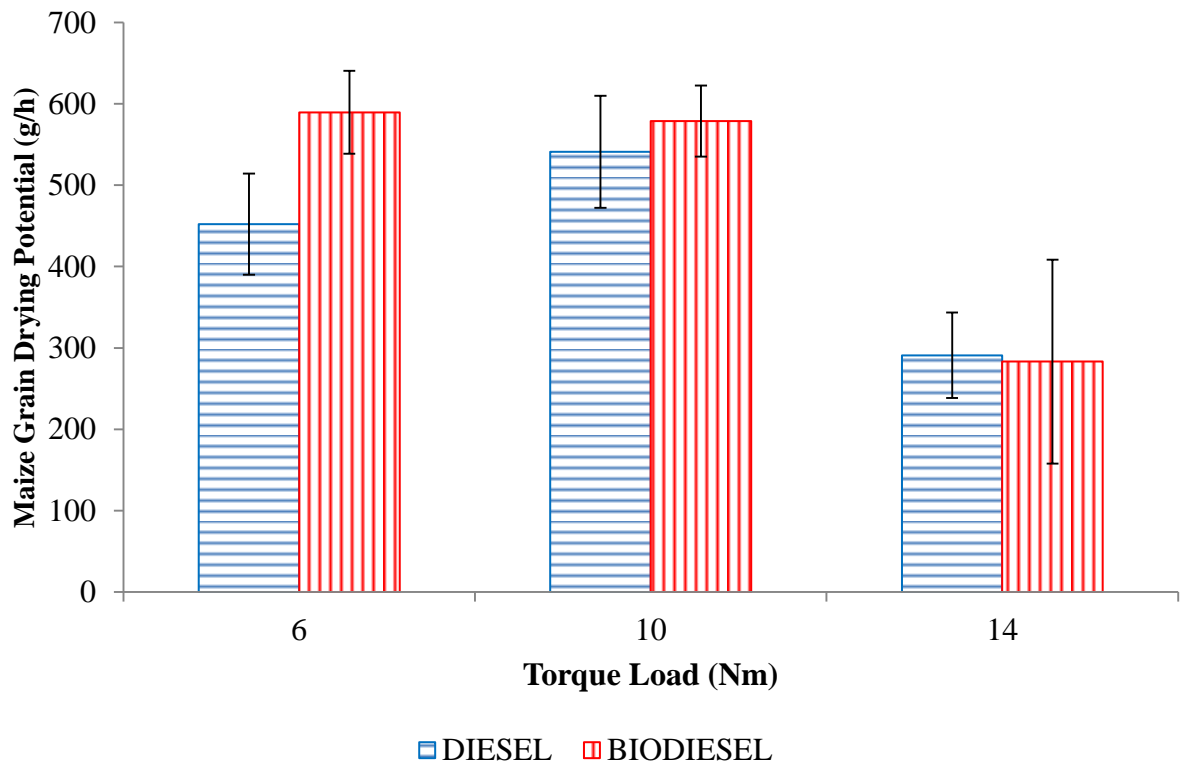


Figure 4. 9: Estimated maize that could be dried against torque load at 1500 rpm

CHAPTER FIVE

CONCLUSIONS AND RECOMMENDATIONS

5.1 Conclusions

This research was set out to recover exhaust gases energy from internal combustion engines for use in other applications. The research used a 3.5 kW single cylinder, four-stroke, multi-fuel engine which was operated on diesel and biodiesel fuels. Farmers have adopted mechanized agriculture and they use tractors from where heat energy is inevitably lost through the exhaust gases. These tractors have engine capacities as high as 120 kW and are about 35 times higher than the capacity of the engine used for this study.

. The specific conclusions drawn from the research are:

- i. Based on this research, the peak thermal energy lost through the exhaust was 7.2% of the fuel energy when the engine was operated on diesel. When the engine used biodiesel the peak thermal energy lost through the exhaust was 16.8% of the fuel energy. The peak heat loss through the exhaust was 21.5% lower when the engine was fueled on diesel than when biodiesel was used at 1500 rpm and 18 Nm. The lost energy increased with increased exhaust gas temperature at higher engine speeds and loads.
- ii. In this study, the maximum recovered energy from the exhaust was 60% of the brake power when the engine was operated on diesel. When the engine used biodiesel the maximum recovered energy from the exhaust was 78% of the brake power. The maximum recovered energy from the exhaust was 29.1% lower when the engine was fueled on diesel than when biodiesel was used at 1000 rpm and 18 Nm. The recovered energy from the exhaust gases increased with increased engine speed and load to an optimum. Energy recovered from the exhaust gases when the engine was operated on biodiesel was more than when the engine used diesel. However, with better and improved energy recovery systems more energy could be recovered.
- iii. Through simulation, specific energy required to dry maize from a moisture content of 25% to 13% wet basis was found to be 1124 kJ/kg. In this study, 750 and 566 grams per hour of maize could be dried when the engine used biodiesel and diesel respectively at an engine speed of 1000 rpm and a load of 18 Nm. With an engine capacity as high as 120 kW, about 25 kg/h of maize could be dried.

5.2 Recommendations

From these research findings, more research work can be done:

- i. More energy was lost through the exhaust gases when the engine was operated on biodiesel than when the engine used diesel. Further research on petrol engines would contribute to more knowledge.
- ii. Recovered energy depended on the recovery method. Thus, there is need to use better and improved energy recovery systems.
- iii. The amount of maize that could be dried with the recovered energy largely depended on the engine capacity. This research used a 3.5 kW engine. There is need for further research using an engine with a higher capacity to verify the upscaled values of the amount of maize that could be dried.

REFERENCES

- Acharyaviriya, S., Soponronnarit, S., & Terdyothin, A. (2000). Mathematical model development and simulation of heat pump fruit dryer. *Drying Technology*, 18(1), 479-491.
- Arias, D. A., Shedd, T. A., & Jester, R. K. (2006). Theoretical analysis of waste heat recovery from an internal combustion engine in a hybrid vehicle: SAE Technical Paper.
- Armstead, J. R., & Miers, S. A. (2014). Review of waste heat recovery mechanisms for internal combustion engines. *Journal of Thermal Science and Engineering Applications*, 6(1), 14-20.
- Aukah, J., Muvengei, M., Ndiritu, H., & Onyango, C. (2015). *Simulation of drying uniformity inside hybrid solar biomass dryer using ANSYS CFX*. Paper presented at the proceedings of sustainable research and innovation conference, in Kenya.
- Baldia, F., Lacourb, S., Danelc, Q., & Larsend, U. (2015). *Dynamic modelling and analysis of the potential for waste heat recovery on diesel engine driven applications with a cyclical operational profile*. Paper presented at the 28th international conference on efficiency, cost, optimization, simulation and environmental impact of energy systems, in France.
- Ban-Weiss, G. A., McLaughlin, J. P., Harley, R. A., Kean, A. J., Grosjean, E., & Grosjean, D. (2008). Carbonyl and nitrogen dioxide emissions from gasoline-and diesel-powered motor vehicles. *Environmental Science and Technology*, 42(11), 3944-3950.
- Basunia, M., & Abe, T. (2008). Performance study of a small engine waste heated bin dryer in deep bed drying of paddy. *Agricultural Engineering International: CIGR Journal*, 3(1), 34-41.
- Basunia, M., Abe, T., & Hikida, Y. (1997). Utilization of engine waste heat for paddy drying and validation of the stationary-bed grain drying model in variable low temperature drying. *Agricultural Mechanization in Asia, Africa and Latin America*, 4(28), 47-52.
- Bhale, P. V., Deshpande, N. V., & Thombre, S. B. (2009). Improving the low temperature properties of biodiesel fuel. *Renewable Energy*, 34(3), 794-800.
- Braun, J., Bansal, P., & Groll, E. (2002). Energy efficiency analysis of air cycle heat pump dryers. *International Journal of Refrigeration*, 25(7), 954-965.
- Canakci, M. (2005). Performance and emissions characteristics of biodiesel from soybean oil. *Journal of Automobile Engineering*, 219(7), 915-922.

- Chauhan, V. (2012). Review of research in mechanical engineering on recovery of waste heat in internal combustion engine. *International Journal of Research in Engineering and Applied Sciences*, 2(12), 2249-3905.
- Conklin, J. C., & Szybist, J. P. (2010). A highly efficient six-stroke internal combustion engine cycle with water injection for in-cylinder exhaust heat recovery. *Energy*, 35(4), 1658-1664.
- Daccord, R., Melis, J., Kientz, T., Darmedru, A., Pireyre, R., Brisseau, N., & Fonteneau, E. (2013). *Exhaust heat recovery with Rankine piston expander*. Paper presented at the proceedings of ICE powertrain electrification and energy recovery, in France.
- Dadi, M., Molvi, I., & Mehta, A. (2012). The most efficient waste heat recovery device: A gamma type stirling engine. *International Journal of Advanced Engineering Technology*, 3(5), 189-195.
- Dincer, I., Hussain, M., Sahin, A., & Yilbas, B. (2002). Development of a new moisture transfer (Bi-Re) correlation for food drying applications. *International Journal of Heat and Mass Transfer*, 45(8), 1749-1755.
- Drescher, U., & Brüggemann, D. (2007). Fluid selection for the organic Rankine cycle (ORC) in biomass power and heat plants. *Applied Thermal Engineering*, 27(1), 223-228.
- Edwards, K. D., Wagner, R., & Briggs, T. (2010). Investigating Potential Light-duty Efficiency Improvements through Simulation of Turbo-compounding and Waste-heat Recovery Systems: SAE International.
- Enderlein, M., Ricoeur, A., & Kuna, M. (2005). Finite element techniques for dynamic crack analysis in piezoelectrics. *International Journal of Fracture*, 134(3), 191-208.
- Endo, T., Kawajiri, S., Kojima, Y., Takahashi, K., Baba, T., Ibaraki, S., Takahashi, T., & Shinohara, M. (2007). Study on maximizing exergy in automotive engines: SAE Technical Paper.
- Espinosa, N., Tilman, L., Lemort, V., Quoilin, S., & Lombard, B. (2010). *Rankine cycle for waste heat recovery on commercial trucks: approach, constraints and modelling*. Paper presented at the diesel international conference and exhibition, in France.
- Feru, E., de Jager, B., Willems, F., & Steinbuch, M. (2014). Two-phase plate-fin heat exchanger modeling for waste heat recovery systems in diesel engines. *Applied Energy*, 133(9), 183-196.

- Feru, E., Kupper, F., Rojer, C., Seykens, X., Scappin, F., Willems, F., Smits, J., De Jager, B., & Steinbuch, M. (2013). Experimental validation of a dynamic waste heat recovery system model for control purposes: SAE Technical Paper.
- Galanis, N., Cayer, E., Roy, P., Denis, E., & Desilets, M. (2009). Electricity generation from low temperature sources. *Journal of Applied Fluid Mechanics*, 2(2), 55-67.
- Ganesan, V. (2012). *Internal combustion engines*: McGraw Hill Education (India) Pvt Ltd.
- Gopal, N. K., Subbarao, R., Pandiyarajan, V., & Velraj, R. (2010). Thermodynamic analysis of a diesel engine integrated with a PCM based energy storage system. *International Journal of Thermodynamics*, 13(1), 15-21.
- Gotmalm, O. (1992). Diesel Exhaust Control: SAE Technical Paper.
- Greszler, A. (2008). *Diesel turbo-compound technology, ICCT*. Paper presented at the NESCCAF workshop for improving fuel economy of heavy-duty fleets.
- Grisso, R., Perumpral, J., & Zoz, F. (2007). Spreadsheet for matching tractors and drawn implements. *Applied Engineering in Agriculture*, 23(3), 259-265.
- Haidar, J. G., & Ghojel, J. I. (2001). *Waste heat recovery from the exhaust of low-power diesel engine using thermoelectric generators*. Paper presented at the proceedings of international conference on thermoelectrics.
- Hansen, K. F., & Jensen, M. G. (1997). Chemical and biological characteristics of exhaust emissions from a DI diesel engine fuelled with rapeseed oil methyl ester (RME): SAE Technical Paper.
- Hashemi, S., Roald, M., & Murray Douglas, W. (2003). Mechanism of through air drying of paper: application in hybrid drying. *Drying technology*, 21(2), 349-368.
- Hatazawa, M., Sugita, H., Ogawa, T., & Seo, Y. (2004). Performance of a thermoacoustic sound wave generator driven with waste heat of automobile gasoline engine. *Transactions of Japan Society of Mechanical Engineers*, 16(1), 292-299.
- Herner, J. D., Hu, S., Robertson, W. H., Huai, T., Collins, J. F., Dwyer, H., & Ayala, A. (2009). Effect of advanced aftertreatment for PM and NO_x control on heavy-duty diesel truck emissions. *Environmental Science and Technology*, 43(15), 5928-5933.
- Heywood, J. (1988). *Internal Combustion Engine Fundamentals*: McGraw-Hill Education.
- Hossain, S. N., & Bari, S. (2011). *Effect of design-parameters of heat exchanger on recovering heat from exhaust of diesel engine using organic Rankine cycle*. Paper presented at the international conference of mechanical engineering, in Dhaka, Bangladesh.

- Hossain, S. N., & Bari, S. (2014). Waste heat recovery from exhaust of a diesel generator set using organic fluids. *Procedia Engineering*, 90(5), 439-444.
- Hounsham, S., Stobart, R., Cooke, A., & Childs, P. (2008). Energy recovery systems for engines: SAE Technical Paper.
- Hountalas, D., Katsanos, C., & Lamaris, V. (2007). Recovering energy from the diesel engine exhaust using mechanical and electrical turbocompounding: SAE Technical Paper.
- Hsiung, M. Y., & Yeh, R. H. (2014). Analyzing the optimization of an organic Rankine cycle system for recovering waste heat from a large marine engine containing a cooling water system. *Energy Conversion and Management*, 88(4), 999-1010.
- Jadhao, J. S., & Thombare, D. G. (2013). Review on exhaust gas heat recovery for IC engine. *International Journal of Engineering and Innovative Technology*, 2(12), 93-100.
- Jia, H., Hong, G., Cheng, N., & Li, W. (2012). *Key techniques for designing free piston stirling engine*. Paper presented at the power and energy engineering conference, in Asia.
- Jiangzhou, S., Wang, R., Lu, Y., Xu, Y., Wu, J., & Li, Z. (2003). Locomotive driver cabin adsorption air-conditioner. *Renewable Energy*, 28(11), 1659-1670.
- Johnson, V. H. (2002). Heat-generated cooling opportunities in vehicles: SAE Technical Paper.
- Kadota, M., & Yamamoto, K. (2008). Advanced transient simulation on hybrid vehicle using Rankine cycle system. *SAE International Journal of Engines*, 1(2), 240-247.
- Kalikatzarakis, M., & Frangopoulos, C. A. (2015). Multi-criteria selection and thermo-economic optimization of organic Rankine cycle system for a marine application. *International Journal of Thermodynamics*, 18(2), 133-141.
- Kalligeros, S., Zannikos, F., Stournas, S., Lois, E., Anastopoulos, G., Teas, C., & Sakellaropoulos, F. (2003). An investigation of using biodiesel/marine diesel blends on the performance of a stationary diesel engine. *Biomass and Bioenergy*, 24(2), 141-149.
- Karaosmanoglu, F. (1999). Vegetable oil fuels: A review. *Energy Sources*, 21(3), 221-231.
- Karathanos, V. T., & Belessiotis, V. G. (1999). Application of a thin-layer equation to drying data of fresh and semi-dried fruits. *Journal of Agricultural Engineering Research*, 74(4), 355-361.
- Karellas, S., Leontaritis, A. D., Panousis, G., Bellos, E., & Kakaras, E. (2013). Energetic and exergetic analysis of waste heat recovery systems in the cement industry. *Energy*, 58(12), 147-156.

- Kong, X., Wang, R., & Huang, X. (2004). Energy efficiency and economic feasibility of CCHP driven by stirling engine. *Energy Conversion and Management*, 45(9), 1433-1442.
- Krokida, M., & Maroulis, Z. (2000). Quality changes during drying of food materials. *Drying Technology in Agriculture and Food Sciences*, 4(2), 61-68.
- Kruiswyk, R. W. (2008). *An engine system approach to exhaust waste heat recovery*. Paper presented at the diesel engine efficiency and emissions research (DEER) conference, in Dearborn.
- Kumar, R. C., Sonthalia, A., & Goel, R. (2011). Experimental study on waste heat recovery from an IC engine using thermoelectric technology. *Thermal Science*, 15(4), 1011-1022.
- Kwankaomeng, S., & Promvongse, P. (2010). *Investigation on a free piston Stirling engine and pneumatic output*. Paper presented at the international conference on mechanical engineering.
- Lacour, S., Descloux, S., Baldi, F., & Podevin, P. (2011). Waste heat recovery on tractor engine: Exergy analysis of exhaust in transient conditions. *Pitesti University Journal*, 21(8), 145-152.
- Larjola, J. (1995). Electricity from industrial waste heat using high speed organic Rankine cycle (ORC). *International Journal of Production Economics*, 41(13), 227-235.
- Leduc, P., & Smague, P. (2013). *Rankine system for heat recovery: An interesting way to reduce fuel consumption*. Paper presented at the proceedings of ICE powertrain electrification and energy recovery, in Rueil-Malmaison, France.
- Lee, Y. R., Kuo, C. R., Liu, C. H., Fu, B. R., Hsieh, J. C., & Wang, C. C. (2014). Dynamic response of a 50 kW organic Rankine cycle system in association with evaporators. *Energies*, 7(4), 2436-2448.
- Lloyd, A. C., & Cackette, T. A. (2001). Diesel engines: Environmental impact and control. *Journal of Air and Waste Management Association*, 51(6), 809-847.
- Magan, N., & Aldred, D. (2007). Post harvest control strategies: Minimizing mycotoxins in the food chain. *International Journal of Food Microbiology*, 119(1), 131-139.
- Mavropoulos, G., & Hountalas, D. (2010). Potential for improving HD diesel truck engine fuel consumption using exhaust heat recovery techniques. In A. Romagnoli & R. F. Martinez-Botas (Eds.), *New trends in technologies: Devices, computer, communication and industrial systems*: InTech.

- McMeeking, R. M. (2004). The energy release rate for a Griffith crack in a piezoelectric material. *Engineering Fracture Mechanics*, 71(7), 1149-1163.
- Milkov, N., Punov, P., Evtimov, T., Descombes, G., & Podevin, P. (2014). *Energy and exergy analysis of an automotive direct injection diesel engine*. Paper presented at the BulTrans scientific conference.
- Miller, E. W., Hendricks, T. J., & Peterson, R. B. (2009). Modeling energy recovery using thermoelectric conversion integrated with an organic Rankine bottoming cycle. *Journal of Electronic Materials*, 38(7), 1206-1213.
- Morales, R. S., Rigola, J., Rodriguez, I., & Oliva, A. (2012). Numerical resolution of the liquid vapour two phase flow by means of the two fluid model and a pressure based method. *International Journal of Multiphase Flow*, 43(10), 118-130.
- Moran, M. J., Shapiro, H. N., Boettner, D. D., & Bailey, M. B. (2010). *Fundamentals of engineering thermodynamics*. New York: John Wiley & Sons.
- Nadaf, S., & Gangavati, P. (2014). A review on waste heat recovery and utilization from diesel engines. *International Journal of Advanced Engineering Technology*, 31(7), 39-45.
- Nam, D. (2000). How to reduce emission of nitrogen oxides (NOx) from marine diesel engines: Annex VI of MARPOL.
- Nelson, C. (2008). *Exhaust energy recovery*. Paper presented at the diesel engine efficiency and emissions research conference, in Dearborn.
- Nielsen, R. F., Haglind, F., & Larsen, U. (2014). Design and modeling of an advanced marine machinery system including waste heat recovery and removal of sulphur oxides. *Energy Conversion and Management*, 85(6), 687-693.
- Özcan, H., & Söylemez, M. (2006). Thermal balance of a LPG fuelled, four stroke SI engine with water addition. *Energy Conversion and Management*, 47(5), 570-581.
- Palmer, R., Wild, D., & Runtz, K. (2003). Improving the efficiency of field operations. *Biosystems Engineering*, 84(3), 283-288.
- Pandiyarajan, V., Pandian, M. C., Malan, E., Velraj, R., & Seeniraj, R. (2011). Experimental investigation on heat recovery from diesel engine exhaust using finned shell and tube heat exchanger and thermal storage system. *Applied Energy*, 88(1), 77-87.
- Punov, P., Lacour, S., Périlhon, C., & Podevin, P. (2013). *Possibilities of waste heat recovery on tractor engines*. Paper presented at the scientific conference on aeronautics, automotive and railway engineering and technologies.

- Quoilin, S., Aumann, R., Grill, A., Schuster, A., Lemort, V., & Spliethoff, H. (2011). Dynamic modeling and optimal control strategy of waste heat recovery using organic Rankine cycles. *Applied Energy*, 88(6), 2183-2190.
- Quoilin, S., Declaye, S., Legros, A., Guillaume, L., & Lemort, V. (2012). *Working fluid selection and operating maps for organic Rankine cycle expansion machines*. Paper presented at the proceedings of the 21st international compressor conference, at Purdue.
- Rahman, S. A., Masjuki, H., Kalam, M., Abedin, M., Sanjid, A., & Sajjad, H. (2013). Impact of idling on fuel consumption and exhaust emissions and available idle reduction technologies for diesel vehicles: A review. *Energy Conversion and Management*, 74(11), 171-182.
- Ringler, J., Seifert, M., Guyotot, V., & Hübner, W. (2009). Rankine cycle for waste heat recovery of IC engines. *SAE International Journal of Engines*, 2(1), 67-76.
- Rubaiyat, S. N. H., & Bari, S. (2010). *Waste heat recovery using shell and tube heat exchanger from the exhaust of an automotive engine*. University of Bangladesh.
- Saidur, R., Rezaei, M., Muzammil, W., Hassan, M., Paria, S., & Hasanuzzaman, M. (2012). Technologies to recover exhaust heat from internal combustion engines. *Renewable and Sustainable Energy Reviews*, 16(8), 5649-5659.
- Saqr, K. M., Mansour, M. K., & Musa, M. N. (2008). Thermal design of automobile exhaust based thermoelectric generators: Objectives and challenges. *International Journal of Automotive Technology*, 9(2), 155-160.
- Sathiamurthi, P. (2011). Design and development of waste heat recovery system for air conditioning. *Unit European Journal of Scientific Research*, 54(1), 102-110.
- Schumacher, L., Frisby, J., & Hires, W. (1991). Tractor PTO horsepower, filter maintenance, and tractor engine oil analysis. *Applied Engineering in Agriculture*, 7(5), 625-629.
- Seher, D., Lengenfelder, T., Gerhardt, J., Eisenmenger, N., Hackner, M., & Krinn, I. (2012). *Waste heat recovery for commercial vehicles with a Rankine process*. Paper presented at the 21st Aachen colloquium on automobile and engine technology, in Aachen, Germany.
- Shahadat, M. M. Z., Nabi, M. N., & Shamim Akhter, M. (2005). *Diesel NOx reduction by preheating inlet air*. Paper presented at the proceedings of the international conference of mechanical engineering.

- Shindo, Y., Murakami, H., Horiguchi, K., & Narita, F. (2002). Evaluation of electric fracture properties of piezoelectric ceramics using the finite element and single edge precracked beam methods. *Journal of American Ceramic Society*, 85(5), 1243-1248.
- Shokati, N., Mohammadkhani, F., Farrokhi, N., & Ranjbar, F. (2014). Thermodynamic and heat transfer analysis of heat recovery from engine test cell by organic Rankine cycle. *Heat and Mass Transfer*, 50(12), 1661-1671.
- Srinivasan, K. K., Mago, P. J., & Krishnan, S. R. (2010). Analysis of exhaust waste heat recovery from a dual fuel low temperature combustion engine using an organic Rankine cycle. *Energy*, 35(6), 2387-2399.
- Stoss, K. J., Sobotzik, J., Shi, B., & Kreis, E. (2013). Tractor power for implement operation: Mechanical, hydraulic, and electrical: An overview: American Society of Agricultural and Biological Engineers.
- Talbi, M., & Agnew, B. (2002). Energy recovery from diesel engine exhaust gases for performance enhancement and air conditioning. *Applied Thermal Engineering*, 22(6), 693-702.
- Talom, H. L., & Beyene, A. (2009). Heat recovery from automotive engine. *Applied Thermal Engineering*, 29(2), 439-444.
- Temos, E. (2006). Using waste heat for energy savings. *ASHRAE Journal*, 48(4), 28-36.
- Teng, H., Regner, G., & Cowland, C. (2007). Waste heat recovery of heavy duty diesel engines by organic Rankine cycle part I: hybrid energy system of diesel and Rankine engines: SAE Technical Paper.
- Van der Hoeven, M. (2012). World energy outlook. Paris: International Energy Agency.
- Vázquez, J., Sanz-Bobi, M. A., Palacios, R., & Arenas, A. (2002). *State of the art thermoelectric generators based on heat recovered from the exhaust gases of automobiles*. Paper presented at the proceedings of the 7th European workshop on thermoelectrics, in Europe.
- Wang, C., & Zhang, C. (2004). *2D and 3D dynamic Green's functions and time-domain BIE formulations for piezoelectric solids*. Paper presented at the proceedings of the WCCM VI in conjunction with APCOM.
- Weerasinghe, W., Stobart, R., & Hounsham, S. (2010). Thermal efficiency improvement in high output diesel engines a comparison of a Rankine cycle with turbocompounding. *Applied Thermal Engineering*, 30(14), 2253-2256.

- Wei, M., Fang, J., Ma, C., & Danish, S. N. (2011). Waste heat recovery from heavy-duty diesel engine exhaust gases by medium temperature ORC system. *China Technological Sciences*, 54(10), 2746-2753.
- Will, F. (2010). *A novel exhaust heat recovery system to reduce fuel consumption*. Paper presented at the proceedings of the world automotive congress.
- Wu, D., & Wang, R. (2006). Combined cooling, heating and power: A review. *Progress in Energy and Combustion Science*, 32(5), 459-495.
- Xiaodong, Z., & Chau, K. (2011). An automotive thermoelectric–photovoltaic hybrid energy system using maximum power point tracking. *Energy Conversion and Management*, 52(1), 641-647.
- Xuejun, H., & Peng, X. (2012). Computational models analysis of diesel engine exhaust waste heat recovery. *Advances in Biomedical Engineering*, 7(3), 228-236.
- Xuyue, W., & Yu, S. (2001). Transient response of a crack in piezoelectric strip subjected to the mechanical and electrical impacts: Mode-I problem. *Mechanics of Materials*, 33(1), 11-20.
- Yuchao, W., Dai, C., & Wang, S. (2013). Theoretical analysis of a thermoelectric generator using exhaust gas of vehicles as heat source. *Applied Energy*, 112(4), 1171-1180.
- Zhang, C., Shu, G., Tian, H., Wei, H., & Liang, X. (2015). Comparative study of alternative ORC-based combined power systems to exploit high temperature waste heat. *Energy Conversion and Management*, 89(5), 541-554.
- Zulkifli, S. A., Karsiti, M. N., & Aziz, A. R. A. (2008). *Starting of a free-piston linear engine-generator by mechanical resonance and rectangular current commutation*. Paper presented at the vehicle power and propulsion conference.

APPENDICES

Appendix A: Tables

Table A 1: Series of notation and description

Notation	Description	Units
N	Engine Speed	rpm
T	Torque Load	Nm
T_i	Exhaust gas temperature before cooling	°C
T_a	Ambient temperature	°C
T_o	Exhaust gas temperature after cooling	°C
\dot{m}_a	Mass flow rate of air	kg/h
\dot{m}_f	Fuel consumption	kg/h
C_p	Specific heat capacity of exhaust gas	kJ/kg°C
\dot{Q}_L	Lost heat energy through exhaust	kJ/h
\dot{Q}_R	Recovered heat energy from exhaust	kJ/h

Table A 2: First observation data at 1000 rpm on diesel fuel

N (rpm)	T (Nm)	T_i (°C)	T_o (°C)	\dot{m}_a (kg/h)	\dot{m}_f (kg/h)
1000	6	227.647	173.102	4.8	0.66
1000	10	242.016	184.192	8.2	0.88
1000	14	273.164	204.718	12.0	0.39
1000	18	317.945	282.369	14.6	1.18
1000	22	323.786	278.953	3.1	1.42

Table A 3: Second observation data at 1000 rpm on diesel fuel

N (rpm)	T (Nm)	T_i (°C)	T_o (°C)	\dot{m}_a (kg/h)	\dot{m}_f (kg/h)
1000	6	211.924	161.631	3.6	1.67
1000	10	227.795	172.493	3.7	1.47
1000	14	249.839	191.050	3.7	1.51
1000	18	287.108	228.235	8.9	0.87
1000	22	318.198	280.754	15.9	0.74

Table A 4: Third observation data at 1000 rpm on diesel fuel

N (rpm)	T (Nm)	T_i (°C)	T_o (°C)	\dot{m}_a (kg/h)	\dot{m}_f (kg/h)
1000	6	239.725	193.337	2.5	0.77
1000	10	241.785	202.019	5.5	1.48
1000	14	267.959	222.986	9.0	1.02
1000	18	320.961	269.417	14.0	1.40
1000	22	311.499	292.197	15.4	1.66

Table A 5: Fourth observation data at 1000 rpm on diesel fuel

N (rpm)	T (Nm)	T_i (°C)	T_o (°C)	\dot{m}_a (kg/h)	\dot{m}_f (kg/h)
1000	6	228.634	196.181	3.70	1.69
1000	10	230.377	196.568	3.63	1.64
1000	14	270.041	217.077	10.29	1.49
1000	18	280.460	228.859	10.10	1.49
1000	22	317.362	268.639	13.81	1.54

Table A 6: First observation data at 1250 rpm on diesel fuel

N (rpm)	T (Nm)	T_i (°C)	T_o (°C)	\dot{m}_a (kg/h)	\dot{m}_f (kg/h)
1250	6	264.848	233.941	7.16	1.94
1250	10	281.045	237.180	7.10	1.49
1250	14	318.459	273.533	6.80	1.72
1250	18	318.375	289.084	9.60	1.78
1250	22	325.045	317.615	6.80	1.92

Table A 7: Second observation data at 1250 rpm on diesel fuel

N (rpm)	T (Nm)	T_i (°C)	T_o (°C)	\dot{m}_a (kg/h)	\dot{m}_f (kg/h)
1250	6	242.431	191.833	7.68	2.61
1250	10	258.738	205.817	8.86	2.28
1250	14	258.607	214.831	12.33	2.42
1250	18	289.268	233.121	10.05	2.47
1250	22	322.694	291.066	19.01	2.36

Table A 8: Third observation data at 1250 rpm on diesel fuel

N (rpm)	T (Nm)	T_i (°C)	T_o (°C)	\dot{m}_a (kg/h)	\dot{m}_f (kg/h)
1250	6	257.528	229.184	4.30	1.60
1250	10	273.392	234.421	4.30	1.43
1250	14	304.717	258.986	4.15	1.79
1250	18	319.384	298.671	12.60	1.27
1250	22	322.229	313.215	14.20	1.28

Table A 9: Fourth observation data at 1250 rpm on diesel fuel

N (rpm)	T (Nm)	T_i (°C)	T_o (°C)	\dot{m}_a (kg/h)	\dot{m}_f (kg/h)
1250	6	243.081	212.699	6.45	1.94
1250	10	250.303	216.472	6.39	2.04
1250	14	249.473	216.427	9.32	1.69
1250	18	320.217	279.187	13.43	1.05
1250	22	327.409	304.220	16.34	1.89

Table A 10: First observation data at 1500 rpm on diesel fuel

N (rpm)	T (Nm)	T_i (°C)	T_o (°C)	\dot{m}_a (kg/h)	\dot{m}_f (kg/h)
1500	6	290.841	260.677	7.56	2.50
1500	10	330.574	283.554	7.12	2.46
1500	14	334.714	299.805	9.43	2.53
1500	18	320.474	-	12.74	2.40
1500	22	300.004	-	16.20	2.31

Table A 11: Second observation data at 1500 rpm on diesel fuel

N (rpm)	T (Nm)	T_i (°C)	T_o (°C)	\dot{m}_a (kg/h)	\dot{m}_f (kg/h)
1500	6	275.075	218.579	7.27	2.66
1500	10	295.660	237.811	11.21	2.42
1500	14	301.225	273.599	13.23	2.46
1500	18	304.161	-	10.15	2.28
1500	22	298.602	-	7.05	2.42

Table A 12: Third observation data at 1500 rpm on diesel fuel

N (rpm)	T (Nm)	T_i (°C)	T_o (°C)	\dot{m}_a (kg/h)	\dot{m}_f (kg/h)
1500	6	295.099	246.668	10.57	0.50
1500	10	320.943	274.806	10.43	0.60
1500	14	325.548	309.413	14.38	0.80
1500	18	317.737	-	18.55	0.95
1500	22	310.774	-	18.74	0.80

Table A 13: Fourth observation data at 1500 rpm on diesel fuel

N (rpm)	T (Nm)	T_i (°C)	T_o (°C)	\dot{m}_a (kg/h)	\dot{m}_f (kg/h)
1500	6	284.516	234.036	11.77	0.50
1500	10	307.574	252.812	11.66	0.55
1500	14	323.626	313.140	18.58	0.85
1500	18	325.890	-	18.56	0.85
1500	22	328.910	-	18.59	0.65

Table A 14: First observation data at 1000 rpm on biodiesel fuel

N (rpm)	T (Nm)	T_i (°C)	T_o (°C)	\dot{m}_a (kg/h)	\dot{m}_f (kg/h)
1000	6	227.619	182.094	4.23	1.69
1000	10	234.139	188.569	6.87	1.40
1000	14	256.046	204.870	9.66	1.59
1000	18	283.127	227.821	11.43	1.80
1000	22	319.657	271.429	15.50	1.70

Table A 15: Second observation data at 1000 rpm on biodiesel fuel

N (rpm)	T (Nm)	T_i (°C)	T_o (°C)	\dot{m}_a (kg/h)	\dot{m}_f (kg/h)
1000	6	215.838	184.081	2.33	1.64
1000	10	225.843	186.420	5.62	1.69
1000	14	269.325	213.808	10.61	1.54
1000	18	319.871	270.279	14.50	0.95
1000	22	328.359	289.753	12.63	1.29

Table A 16: Third observation data at 1000 rpm on biodiesel fuel

N (rpm)	T (Nm)	T_i (°C)	T_o (°C)	\dot{m}_a (kg/h)	\dot{m}_f (kg/h)
1000	6	222.326	180.848	3.67	1.74
1000	10	224.081	184.302	3.71	1.69
1000	14	256.476	203.307	10.76	1.44
1000	18	303.970	239.555	13.18	1.44
1000	22	318.208	261.205	14.90	1.34

Table A 17: Fourth observation data at 1000 rpm on biodiesel fuel

N (rpm)	T (Nm)	T_i (°C)	T_o (°C)	\dot{m}_a (kg/h)	\dot{m}_f (kg/h)
1000	6	217.077	178.117	3.09	1.44
1000	10	235.485	189.174	7.18	1.49
1000	14	278.860	216.577	12.24	1.05
1000	18	315.206	258.728	14.49	1.59
1000	22	328.367	283.987	5.19	1.54

Table A 18: First observation data at 1250 rpm on biodiesel fuel

N (rpm)	T (Nm)	T_i (°C)	T_o (°C)	\dot{m}_a (kg/h)	\dot{m}_f (kg/h)
1250	6	247.414	187.366	8.88	1.99
1250	10	280.388	225.289	11.01	1.89
1250	14	305.385	256.624	14.27	1.99
1250	18	317.418	284.402	16.46	1.84
1250	22	333.043	319.782	17.20	2.04

Table A 19: Second observation data at 1250 rpm on biodiesel fuel

N (rpm)	T (Nm)	T_i (°C)	T_o (°C)	\dot{m}_a (kg/h)	\dot{m}_f (kg/h)
1250	6	246.800	214.425	6.87	2.09
1250	10	255.045	220.035	6.47	2.04
1250	14	277.346	232.894	10.65	1.94
1250	18	321.694	278.270	14.73	1.89
1250	22	330.843	312.229	15.92	1.89

Table A 20: Third observation data at 1250 rpm on biodiesel fuel

N (rpm)	T (Nm)	T_i (°C)	T_o (°C)	\dot{m}_a (kg/h)	\dot{m}_f (kg/h)
1250	6	245.630	212.248	6.61	2.19
1250	10	249.447	214.568	6.41	1.99
1250	14	293.036	243.224	12.03	2.04
1250	18	325.270	284.083	15.10	2.09
1250	22	329.513	318.898	17.28	1.94

Table A 21: Fourth observation data at 1250 rpm on biodiesel fuel

N (rpm)	T (Nm)	T_i (°C)	T_o (°C)	\dot{m}_a (kg/h)	\dot{m}_f (kg/h)
1250	6	240.367	199.701	6.98	2.14
1250	10	243.740	204.790	8.05	1.89
1250	14	274.938	225.249	11.21	1.99
1250	18	311.435	260.138	14.11	1.94
1250	22	330.683	301.111	16.77	2.04

Table A 22: First observation data at 1500 rpm on biodiesel fuel

N (rpm)	T (Nm)	T_i (°C)	T_o (°C)	\dot{m}_a (kg/h)	\dot{m}_f (kg/h)
1500	6	292.606	230.947	11.40	0.50
1500	10	327.868	274.213	11.08	0.65
1500	14	332.566	293.729	14.18	0.80
1500	18	325.557	-	18.79	0.95
1500	22	307.116	-	18.33	2.14

Table A 23: Second observation data at 1500 rpm on biodiesel fuel

N (rpm)	T (Nm)	T_i (°C)	T_o (°C)	\dot{m}_a (kg/h)	\dot{m}_f (kg/h)
1500	6	296.556	246.940	12.22	0.50
1500	10	331.026	288.427	11.97	0.70
1500	14	329.034	325.007	18.82	0.85
1500	18	321.619	-	18.89	0.95
1500	22	310.916	-	18.70	1.05

Table A 24: Third observation data at 1500 rpm on biodiesel fuel

N (rpm)	T (Nm)	T_i (°C)	T_o (°C)	\dot{m}_a (kg/h)	\dot{m}_f (kg/h)
1500	6	302.282	262.218	12.22	0.50
1500	10	329.779	291.089	15.82	0.70
1500	14	330.055	310.591	18.79	0.70
1500	18	328.370	-	18.77	0.85
1500	22	324.903	-	18.74	0.95

Table A 25: Fourth observation data at 1500 rpm on biodiesel fuel

N (rpm)	T (Nm)	T_i (°C)	T_o (°C)	\dot{m}_a (kg/h)	\dot{m}_f (kg/h)
1500	6	300.681	239.919	2.33	1.64
1500	10	318.447	261.506	5.62	1.69
1500	14	330.696	311.114	10.61	1.54
1500	18	319.077	-	18.82	1.00
1500	22	331.005	-	18.84	0.80

Table A 26: Heat energy lost and recovered at 1000 rpm and 6 Nm for diesel fuel

\dot{m}_a (kg/h)	\dot{m}_f (kg/h)	C_p (kJ/kg°C)	T_i (°C)	T_a (°C)	T_o (°C)	\dot{Q}_L (kJ/h)	\dot{Q}_R (kJ/h)
4.8	0.66	1.006	227.647	24	173.102	1118.584	299.603
3.6	1.67	1.006	211.924	24	161.631	996.302	266.634
2.5	0.77	1.006	239.725	24	193.337	709.653	152.599
3.7	1.69	1.006	228.634	24	196.181	1109.595	175.971
Mean						983.534	223.702
Standard deviation						190.878	70.564
Standard error from mean						95.439	35.282

Table A 27: Heat energy lost and recovered at 1000 rpm and 10 Nm for diesel fuel

\dot{m}_a (kg/h)	\dot{m}_f (kg/h)	C_p (kJ/kg°C)	T_i (°C)	T_a (°C)	T_o (°C)	\dot{Q}_L (kJ/h)	\dot{Q}_R (kJ/h)
3.70	1.47	1.006	227.795	24	172.493	1059.942	287.627
8.20	0.88	1.006	242.016	24	184.192	1991.463	528.192
5.50	1.48	1.006	241.785	24	202.019	1529.260	279.232
3.63	1.64	1.006	230.377	24	196.568	1094.132	179.242
Mean						1418.699	318.573
Standard deviation						437.543	148.165
Standard error from mean						218.772	74.082

Table A 28: Heat energy lost and recovered at 1000 rpm and 14 Nm for diesel fuel

\dot{m}_a (kg/h)	\dot{m}_f (kg/h)	C_P (kJ/kg°C)	T_i (°C)	T_a (°C)	T_o (°C)	\dot{Q}_L (kJ/h)	\dot{Q}_R (kJ/h)
9.00	1.02	1.006	267.959	24	222.986	2459.136	453.333
12.00	0.39	1.006	273.164	24	204.718	3105.665	853.134
3.70	1.51	1.006	249.839	24	191.050	1183.681	308.128
10.29	1.49	1.006	270.041	24	217.077	2915.753	627.659
Mean						2416.059	560.564
Standard deviation						865.229	234.749
Standard error from mean						432.614	117.374

Table A 29: Heat energy lost and recovered at 1000 rpm and 18 Nm for diesel fuel

\dot{m}_a (kg/h)	\dot{m}_f (kg/h)	C_P (kJ/kg°C)	T_i (°C)	T_a (°C)	T_o (°C)	\dot{Q}_L (kJ/h)	\dot{Q}_R (kJ/h)
10.1	1.49	1.006	280.460	24	228.859	2990.206	601.644
14.6	1.18	1.006	317.945	24	282.369	4666.283	564.758
8.9	0.87	1.006	287.108	24	228.235	2585.989	578.640
14.1	1.40	1.006	320.961	24	269.417	4600.639	798.540
Mean						3710.779	635.896
Standard deviation						1078.458	109.492
Standard error from mean						539.229	54.746

Table A 30: Heat energy lost and recovered at 1000 rpm and 22 Nm for diesel fuel

\dot{m}_a (kg/h)	\dot{m}_f (kg/h)	C_P (kJ/kg°C)	T_i (°C)	T_a (°C)	T_o (°C)	\dot{Q}_L (kJ/h)	\dot{Q}_R (kJ/h)
3.10	1.42	1.006	323.786	24	278.953	1363.163	203.861
15.90	0.74	1.006	318.198	24	280.754	4924.827	626.807
15.40	1.66	1.006	311.499	24	292.197	4934.161	331.268
13.81	1.54	1.006	317.362	24	268.639	4530.125	752.385
Mean						3938.069	478.580
Standard deviation						1726.901	254.370
Standard error from mean						863.451	127.185

Table A 31: Heat energy lost and recovered at 1250 rpm and 6 Nm for diesel fuel

\dot{m}_a (kg/h)	\dot{m}_f (kg/h)	C_P (kJ/kg°C)	T_i (°C)	T_a (°C)	T_o (°C)	\dot{Q}_L (kJ/h)	\dot{Q}_R (kJ/h)
7.16	1.94	1.006	264.848	24	233.941	2204.867	282.941
7.68	2.61	1.006	242.431	24	191.833	2261.141	523.777
4.30	1.60	1.006	257.528	24	229.184	1386.082	168.233
6.45	1.94	1.006	243.081	24	212.699	1849.118	256.434
Mean						1925.302	307.846
Standard deviation						403.116	152.076
Standard error from mean						201.558	76.038

Table A 32: Heat energy lost and recovered at 1250 rpm and 10 Nm for diesel fuel

\dot{m}_a (kg/h)	\dot{m}_f (kg/h)	C_P (kJ/kg°C)	T_i (°C)	T_a (°C)	T_o (°C)	\dot{Q}_L (kJ/h)	\dot{Q}_R (kJ/h)
7.10	1.49	1.006	281.045	24	237.180	2221.265	379.061
8.86	2.28	1.006	258.738	24	205.817	2630.671	593.077
6.39	2.04	1.006	250.303	24	216.472	1919.181	286.907
4.30	1.43	1.006	273.392	24	234.421	1437.590	224.644
Mean						2052.177	370.922
Standard deviation						502.875	161.116
Standard error from mean						251.438	80.558

Table A 33: Heat energy lost and recovered at 1250 rpm and 14 Nm for diesel fuel

\dot{m}_a (kg/h)	\dot{m}_f (kg/h)	C_P (kJ/kg°C)	T_i (°C)	T_a (°C)	T_o (°C)	\dot{Q}_L (kJ/h)	\dot{Q}_R (kJ/h)
6.80	1.72	1.006	318.459	24	273.533	2523.843	385.066
12.33	2.42	1.006	258.607	24	214.831	3481.216	649.570
9.32	1.69	1.006	249.473	24	216.427	2497.352	366.019
4.15	1.79	1.006	304.717	24	258.986	1677.464	273.272
Mean						2544.969	418.482
Standard deviation						737.527	161.613
Standard error from mean						368.763	80.807

Table A 34: Heat energy lost and recovered at 1250 rpm and 18 Nm for diesel fuel

\dot{m}_a (kg/h)	\dot{m}_f (kg/h)	C_P (kJ/kg°C)	T_i (°C)	T_a (°C)	T_o (°C)	\dot{Q}_L (kJ/h)	\dot{Q}_R (kJ/h)
9.60	1.78	1.006	318.375	24	289.084	3370.087	335.332
10.05	2.47	1.006	289.268	24	233.121	3341.082	707.178
12.60	1.27	1.006	319.384	24	298.671	4121.558	289.013
13.43	1.05	1.006	320.217	24	279.187	4314.957	597.679
Mean						3786.921	482.300
Standard deviation						504.423	202.355
Standard error from mean						252.211	101.177

Table A 35: Heat energy lost and recovered at 1250 rpm and 22 Nm for diesel fuel

\dot{m}_a (kg/h)	\dot{m}_f (kg/h)	C_P (kJ/kg°C)	T_i (°C)	T_a (°C)	T_o (°C)	\dot{Q}_L (kJ/h)	\dot{Q}_R (kJ/h)
6.80	1.92	1.006	325.045	24	317.615	2640.863	65.178
19.01	2.36	1.006	322.694	24	291.066	6421.389	679.946
14.20	1.28	1.006	322.229	24	313.215	4644.284	140.374
16.34	1.89	1.006	327.409	24	304.220	5564.333	425.272
Mean						4817.717	327.692
Standard deviation						1622.547	281.428
Standard error from mean						811.273	140.714

Table A 36: Heat energy lost and recovered at 1500 rpm and 6 Nm for diesel fuel

\dot{m}_a (kg/h)	\dot{m}_f (kg/h)	C_P (kJ/kg°C)	T_i (°C)	T_a (°C)	T_o (°C)	\dot{Q}_L (kJ/h)	\dot{Q}_R (kJ/h)
7.56	2.50	1.006	290.841	24	260.677	2700.527	305.271
7.27	2.66	1.006	275.075	24	218.579	2508.134	564.371
10.57	0.50	1.006	295.099	24	246.668	3019.072	539.348
11.77	0.50	1.006	284.516	24	234.036	3215.711	623.106
Mean						2860.861	508.024
Standard deviation						316.793	139.653
Standard error from mean						158.396	69.827

Table A 37: Heat energy lost and recovered at 1500 rpm and 10 Nm for diesel fuel

\dot{m}_a (kg/h)	\dot{m}_f (kg/h)	C_P (kJ/kg°C)	T_i (°C)	T_a (°C)	T_o (°C)	\dot{Q}_L (kJ/h)	\dot{Q}_R (kJ/h)
7.12	2.46	1.006	330.574	24	283.554	2954.601	453.154
11.21	2.42	1.006	295.660	24	237.811	3724.942	793.213
10.43	0.60	1.006	320.943	24	274.806	3294.933	511.944
11.66	0.55	1.006	307.574	24	252.812	3483.213	672.656
Mean						3364.422	607.742
Standard deviation						324.997	154.583
Standard error from mean						162.498	77.292

Table A 38: Heat energy lost and recovered at 1500 rpm and 14 Nm for diesel fuel

\dot{m}_a (kg/h)	\dot{m}_f (kg/h)	C_P (kJ/kg°C)	T_i (°C)	T_a (°C)	T_o (°C)	\dot{Q}_L (kJ/h)	\dot{Q}_R (kJ/h)
9.43	2.53	1.006	334.714	24	299.805	3738.436	420.017
13.23	2.46	1.006	301.225	24	273.599	4375.758	436.053
14.38	0.80	1.006	325.548	24	309.413	4604.964	246.399
18.58	0.85	1.006	323.626	24	313.14	5856.664	204.965
Mean						4643.955	326.858
Standard deviation						887.708	118.228
Standard error from mean						443.854	59.114

Table A 39: Heat energy lost and recovered at 1500 rpm and 18 Nm for diesel fuel

\dot{m}_a (kg/h)	\dot{m}_f (kg/h)	C_P (kJ/kg°C)	T_i (°C)	T_a (°C)	T_o (°C)	\dot{Q}_L (kJ/h)	\dot{Q}_R (kJ/h)
12.74	2.40	1.006	320.474	24	-	4515.548	-
10.15	2.28	1.006	304.161	24	-	3503.296	-
18.55	0.95	1.006	317.737	24	-	5762.239	-
18.56	0.85	1.006	325.890	24	-	5894.843	-
Mean						4918.981	-
Standard deviation						1129.943	-
Standard error from mean						564.971	-

Table A 40: Heat energy lost and recovered at 1500 rpm and 22 Nm for diesel fuel

\dot{m}_a (kg/h)	\dot{m}_f (kg/h)	C_P (kJ/kg°C)	T_i (°C)	T_a (°C)	T_o (°C)	\dot{Q}_L (kJ/h)	\dot{Q}_R (kJ/h)
16.20	2.31	1.006	300.004	24	-	5139.487	-
7.05	2.42	1.006	298.602	24	-	2616.084	-
18.74	0.80	1.006	310.774	24	-	5637.185	-
18.59	0.65	1.006	328.910	24	-	5901.667	-
			Mean			4823.606	-
			Standard deviation			1505.220	-
			Standard error from mean			752.610	-

Table A 41: Heat energy lost and recovered at 1000 rpm and 6 Nm for biodiesel fuel

\dot{m}_a (kg/h)	\dot{m}_f (kg/h)	C_P (kJ/kg°C)	T_i (°C)	T_a (°C)	T_o (°C)	\dot{Q}_L (kJ/h)	\dot{Q}_R (kJ/h)
4.23	1.69	1.006	227.619	24	182.094	1212.657	271.125
2.33	1.64	1.006	215.838	24	184.081	766.166	126.832
3.67	1.74	1.006	222.326	24	180.848	1079.381	225.742
3.09	1.44	1.006	217.077	24	178.117	879.887	177.548
			Mean			984.523	200.312
			Standard deviation			199.726	62.126
			Standard error from mean			99.863	31.063

Table A 42: Heat energy lost and recovered at 1000 rpm and 10 Nm for biodiesel fuel

\dot{m}_a (kg/h)	\dot{m}_f (kg/h)	C_P (kJ/kg°C)	T_i (°C)	T_a (°C)	T_o (°C)	\dot{Q}_L (kJ/h)	\dot{Q}_R (kJ/h)
6.87	1.40	1.006	234.139	24	188.569	1748.277	379.125
5.62	1.69	1.006	225.843	24	186.420	1484.325	289.911
3.71	1.69	1.006	224.081	24	184.302	1086.920	216.095
7.18	1.49	1.006	235.485	24	189.174	1844.576	403.925
			Mean			1541.025	322.264
			Standard deviation			338.882	86.062
			Standard error from mean			169.441	43.031

Table A 43: Heat energy lost and recovered at 1000 rpm and 14 Nm for biodiesel fuel

\dot{m}_a (kg/h)	\dot{m}_f (kg/h)	C_P (kJ/kg°C)	T_i (°C)	T_a (°C)	T_o (°C)	\dot{Q}_L (kJ/h)	\dot{Q}_R (kJ/h)
9.66	1.59	1.006	256.046	24	204.870	2626.181	579.184
10.61	1.54	1.006	269.325	24	213.808	2998.583	678.579
10.76	1.44	1.006	256.476	24	203.307	2853.224	652.554
12.24	1.05	1.006	278.860	24	216.577	3407.412	832.708
Mean						2971.350	685.756
Standard deviation						328.627	106.624
Standard error from mean						164.314	53.312

Table A 44: Heat energy lost and recovered at 1000 rpm and 18 Nm for biodiesel fuel

\dot{m}_a (kg/h)	\dot{m}_f (kg/h)	C_P (kJ/kg°C)	T_i (°C)	T_a (°C)	T_o (°C)	\dot{Q}_L (kJ/h)	\dot{Q}_R (kJ/h)
11.43	1.80	1.006	283.127	24	227.821	3448.820	736.089
14.50	0.95	1.006	319.871	24	270.279	4598.634	770.794
13.18	1.44	1.006	303.970	24	239.555	4117.720	947.398
14.49	1.59	1.006	315.206	24	258.728	4710.688	913.615
Mean						4218.966	841.974
Standard deviation						574.257	104.123
Standard error from mean						287.129	52.062

Table A 45: Heat energy lost and recovered at 1000 rpm and 22 Nm for biodiesel fuel

\dot{m}_a (kg/h)	\dot{m}_f (kg/h)	C_P (kJ/kg°C)	T_i (°C)	T_a (°C)	T_o (°C)	\dot{Q}_L (kJ/h)	\dot{Q}_R (kJ/h)
15.50	1.70	1.006	319.657	24	271.429	5115.812	834.499
12.63	1.29	1.006	328.359	24	289.753	4262.097	540.620
14.90	1.34	1.006	318.208	24	261.205	4806.606	931.283
5.19	1.54	1.006	328.367	24	283.987	2060.680	300.469
Mean						4061.299	651.718
Standard deviation						1379.647	287.103
Standard error from mean						689.823	143.551

Table A 46: Heat energy lost and recovered at 1250 rpm and 6 Nm for biodiesel fuel

\dot{m}_a (kg/h)	\dot{m}_f (kg/h)	C_P (kJ/kg°C)	T_i (°C)	T_a (°C)	T_o (°C)	\dot{Q}_L (kJ/h)	\dot{Q}_R (kJ/h)
8.88	1.99	1.006	247.414	24	187.366	2443.081	656.638
6.87	2.09	1.006	246.800	24	214.425	2008.266	291.820
6.61	2.19	1.006	245.630	24	212.248	1962.046	295.524
6.98	2.14	1.006	240.367	24	199.701	1985.107	373.099
Mean						2099.625	404.270
Standard deviation						229.747	172.368
Standard error from mean						114.874	86.184

Table A 47: Heat energy lost and recovered at 1250 rpm and 10 Nm for biodiesel fuel

\dot{m}_a (kg/h)	\dot{m}_f (kg/h)	C_P (kJ/kg°C)	T_i (°C)	T_a (°C)	T_o (°C)	\dot{Q}_L (kJ/h)	\dot{Q}_R (kJ/h)
6.47	2.04	1.006	255.045	24	220.035	1977.990	299.723
11.01	1.89	1.006	280.388	24	225.289	3327.250	715.042
6.41	1.99	1.006	249.447	24	214.568	1905.117	294.742
8.05	1.89	1.006	243.740	24	204.790	2197.321	389.486
Mean						2351.919	424.748
Standard deviation						661.973	198.366
Standard error from mean						330.987	99.183

Table A 48: Heat energy lost and recovered at 1250 rpm and 14 Nm for biodiesel fuel

\dot{m}_a (kg/h)	\dot{m}_f (kg/h)	C_P (kJ/kg°C)	T_i (°C)	T_a (°C)	T_o (°C)	\dot{Q}_L (kJ/h)	\dot{Q}_R (kJ/h)
12.03	2.04	1.006	293.036	24	243.224	3808.049	705.060
14.27	1.99	1.006	305.385	24	256.624	4602.772	797.611
10.65	1.94	1.006	277.346	24	232.894	3208.764	563.009
11.21	1.99	1.006	274.938	24	225.249	3332.256	659.830
Mean						3737.960	681.377
Standard deviation						631.785	97.548
Standard error from mean						315.892	48.774

Table A 49: Heat energy lost and recovered at 1250 rpm and 18 Nm for biodiesel fuel

\dot{m}_a (kg/h)	\dot{m}_f (kg/h)	C_P (kJ/kg°C)	T_i (°C)	T_a (°C)	T_o (°C)	\dot{Q}_L (kJ/h)	\dot{Q}_R (kJ/h)
14.11	1.94	1.006	311.435	24	260.138	4641.012	828.257
16.46	1.84	1.006	317.418	24	284.402	5401.767	607.818
14.73	1.89	1.006	321.694	24	278.270	4977.360	726.037
15.10	2.09	1.006	325.270	24	284.083	5209.904	712.253
Mean						5057.511	718.591
Standard deviation						327.430	90.172
Standard error from mean						163.715	45.086

Table A 50: Heat energy lost and recovered at 1250 rpm and 22 Nm for biodiesel fuel

\dot{m}_a (kg/h)	\dot{m}_f (kg/h)	C_P (kJ/kg°C)	T_i (°C)	T_a (°C)	T_o (°C)	\dot{Q}_L (kJ/h)	\dot{Q}_R (kJ/h)
17.20	2.04	1.006	333.043	24	319.782	5981.663	256.672
15.92	1.89	1.006	330.843	24	312.229	5497.663	333.504
17.28	1.94	1.006	329.513	24	318.898	5907.192	205.244
16.77	2.04	1.006	330.683	24	301.111	5803.319	559.587
Mean						5797.459	338.752
Standard deviation						212.826	156.372
Standard error from mean						106.413	78.186

Table A 51: Heat energy lost and recovered at 1500 rpm and 6 Nm for biodiesel fuel

\dot{m}_a (kg/h)	\dot{m}_f (kg/h)	C_P (kJ/kg°C)	T_i (°C)	T_a (°C)	T_o (°C)	\dot{Q}_L (kJ/h)	\dot{Q}_R (kJ/h)
11.40	0.5	1.006	292.606	24	230.947	3215.590	738.145
12.22	0.5	1.006	296.556	24	246.940	3487.714	634.902
12.22	0.5	1.006	302.282	24	262.218	3560.986	512.672
11.99	0.5	1.006	300.681	24	239.919	3476.480	763.471
Mean						3435.192	662.297
Standard deviation						151.121	114.203
Standard error from mean						75.560	57.102

Table A 52: Heat energy lost and recovered at 1500 rpm and 10 Nm for biodiesel fuel

\dot{m}_a (kg/h)	\dot{m}_f (kg/h)	C_p (kJ/kg°C)	T_i (°C)	T_a (°C)	T_o (°C)	\dot{Q}_L (kJ/h)	\dot{Q}_R (kJ/h)
11.97	0.70	1.006	331.026	24	288.427	3913.360	542.968
11.08	0.65	1.006	327.868	24	274.213	3585.758	633.149
15.82	0.70	1.006	329.779	24	291.089	5081.778	642.994
13.04	0.60	1.006	318.447	24	261.506	4040.355	781.335
Mean						4155.312	650.112
Standard deviation						646.655	98.383
Standard error from mean						323.327	49.192

Table A 53: Heat energy lost and recovered at 1500 rpm and 14 Nm for biodiesel fuel

\dot{m}_a (kg/h)	\dot{m}_f (kg/h)	C_p (kJ/kg°C)	T_i (°C)	T_a (°C)	T_o (°C)	\dot{Q}_L (kJ/h)	\dot{Q}_R (kJ/h)
18.79	0.70	1.006	330.055	24	310.591	6000.802	381.629
14.18	0.80	1.006	332.566	24	293.729	4650.053	585.269
18.82	0.85	1.006	329.034	24	325.007	6036.019	79.686
18.70	0.85	1.006	330.696	24	311.114	6031.882	385.125
Mean						5679.689	357.927
Standard deviation						686.604	208.490
Standard error from mean						343.302	104.245

Table A 54: Heat energy lost and recovered at 1500 rpm and 18 Nm for biodiesel fuel

\dot{m}_a (kg/h)	\dot{m}_f (kg/h)	C_p (kJ/kg°C)	T_i (°C)	T_a (°C)	T_o (°C)	\dot{Q}_L (kJ/h)	\dot{Q}_R (kJ/h)
18.82	1.00	1.006	319.077	24	-	5883.517	-
18.79	0.95	1.006	325.557	24	-	5988.452	-
18.89	0.95	1.006	321.619	24	-	5940.190	-
18.77	0.85	1.006	328.370	24	-	6007.570	-
Mean						5954.932	-
Standard deviation						55.413	-
Standard error from mean						27.706	-

Table A 55: Heat energy lost and recovered at 1500 rpm and 22 Nm for biodiesel fuel

\dot{m}_a (kg/h)	\dot{m}_f (kg/h)	C_p (kJ/kg°C)	T_i (°C)	T_a (°C)	T_o (°C)	\dot{Q}_L (kJ/h)	\dot{Q}_R (kJ/h)
18.70	1.05	1.006	310.916	24	-	5700.591	-
18.74	0.95	1.006	324.903	24	-	5960.329	-
18.33	2.14	1.006	307.116	24	-	5830.157	-
18.84	0.80	1.006	331.005	24	-	6065.756	-
			Mean			5889.208	-
			Standard deviation			158.420	-
			Standard error from mean			79.210	-

Appendix B: Figures

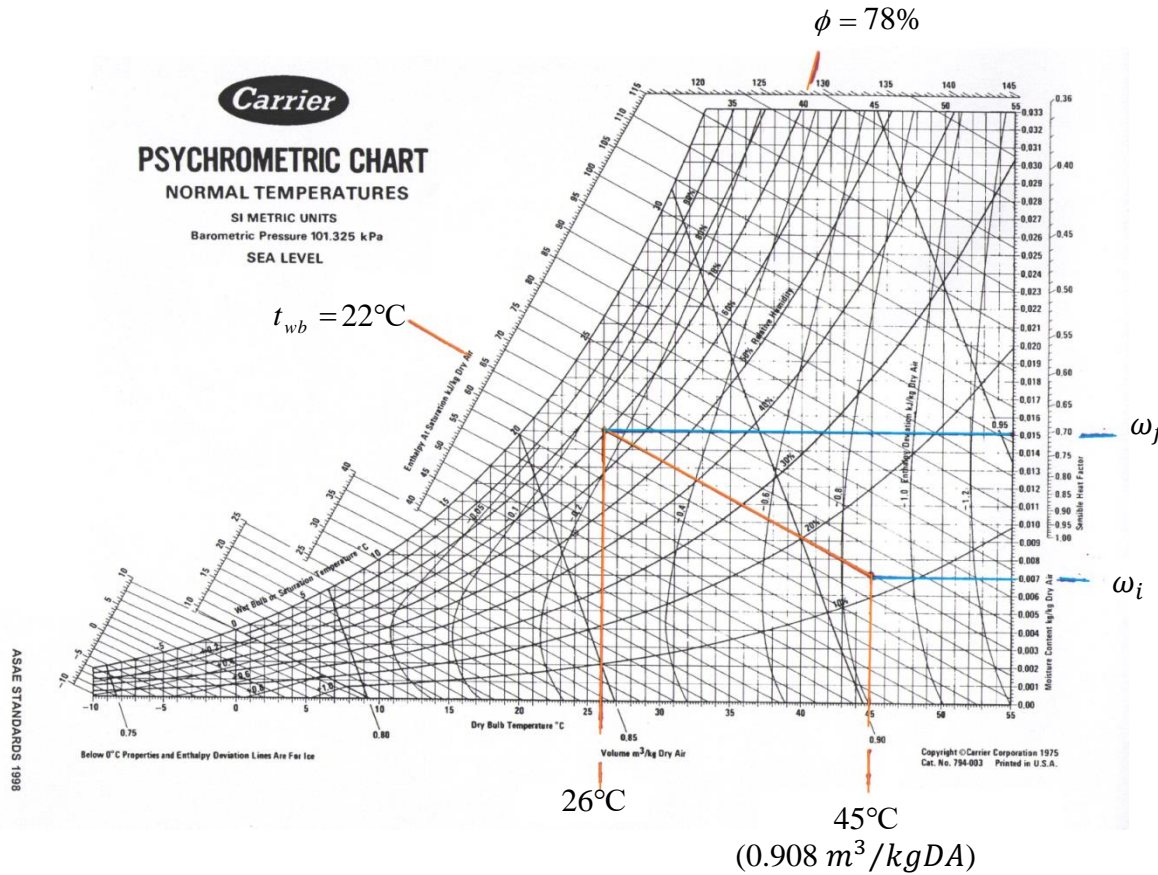


Figure B 1: Psychrometric chart showing drying air entry and exit

Sample calculation for specific energy to dry maize

Rated capacity of dryer = 1900 kg/h

$T_i = 45^\circ\text{C}$ (Drying air entry)

$t_{wb} = 12\%$ (Entrance relative humidity)

$T_o = 26^\circ\text{C}$ (Drying air exit)

$t_{wb} = 78\%$ (Exit relative humidity)

$m_i = 25\%$ wb

$m_f = 13\%$ wb

$$M_i (db) = \frac{m_i (wb)}{1 - m_i (wb)} = 33.3\%$$

$$M_f (db) = \frac{m_f (wb)}{1 - m_f (wb)} = 14.9\%$$

$$\dot{m}_{wi} = \text{Rated capacity} \times m_i (wb) = 475 \text{ kgH}_2\text{O/h}$$

$$\dot{m}_{dmi} = \dot{m}_{dmf} = \text{Rated capacity} - \dot{m}_{wi} = 1425 \text{ kgdm/h}$$

$$\dot{m}_{wf} = \dot{m}_{dmf} \times M_f (db) = 212.325 \text{ kgH}_2\text{O/h}$$

$$\Delta \dot{m}_w = \dot{m}_{wi} - \dot{m}_{wf} = 262.675 \text{ kgH}_2\text{O/h}$$

$$\Delta \omega = \omega_f - \omega_i = 0.008 \text{ kgH}_2\text{O/kgDA}$$

$$\dot{m}_{DA} = \frac{\Delta \dot{m}_w}{\Delta \omega} = 32834.375 \text{ kgDA/h}$$

$$\dot{Q}_r = \frac{h \times \dot{m}_{DA}}{\text{Rated capacity}} = 1123.28 \text{ kJ/kg}$$



Figure B 2: Research engine test setup



Figure B 3: Calorimeter for energy recovery

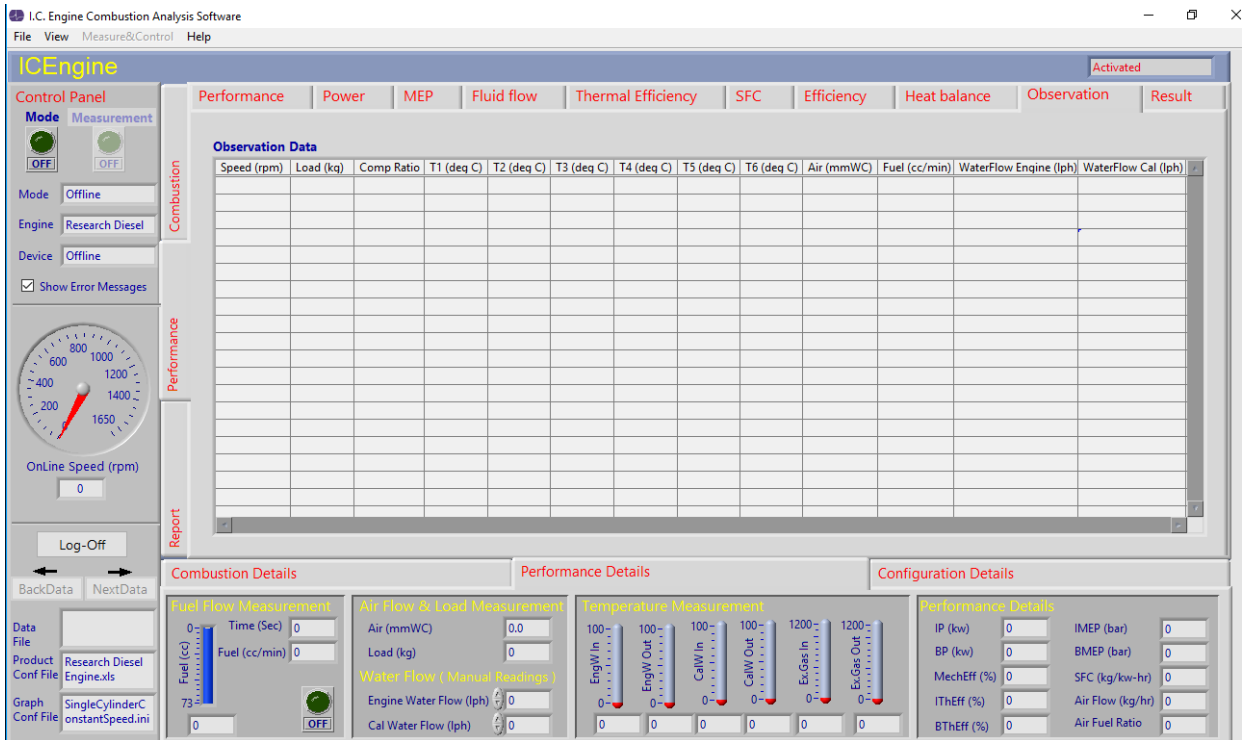


Figure B 4: User interface for ICE analysis software



Figure B 5: Engine fueling

Appendix C: List of Published Articles

Serial number	Description of article
1	Orido, G. O., Ngunjiri, G. M., & Njue, M. R. (2017). Exhaust Gases Energy Recovered from Internal Combustion Engine for Useful Applications. <i>IOSR Journal of Mechanical and Civil Engineering</i> , 14(3), 1-7.
2	Orido, G. O., Ngunjiri, G. M., & Njue, M. R. (2017). Comparison of Thermal Energy Lost through Exhaust Gases at Various Engine Speeds and Torque Loads for Diesel and Biodiesel Fuels. <i>IOSR Journal of Mechanical and Civil Engineering</i> , 14(3), 8-12.
3	Orido, G. O., Njue, M. R., & Ngunjiri, G. M. (2017). Grain Drying Simulation in a GT-380 Dryer using Energy Recovered from ICE Exhaust. <i>IOSR Journal of Agriculture and Veterinary Science</i> , 10(6), 1-6.

Appendix D: Research Authorization Documents


REPUBLIC OF KENYA


**National Commission for Science,
Technology and Innovation**

**RESEACH CLEARANCE
PERMIT**

**Applicant's
Signature**

Serial No. A1655

CONDITIONS: see back page

**THIS IS TO CERTIFY THAT:
MR. GEORGE ONYANGO ORIDO
of EGERTON UNIVERSITY, 0-20115
Nakuru, has been permitted to conduct
research in Nairobi, Nakuru Counties
on the topic: **'EXHAUST GASES ENERGY
RECOVERABLE FROM A DIESEL ENGINE
FOR MAIZE GRAIN DRYING**
for the period ending:
7th November, 2017**

CONDITIONS

1. You must report to the County Commissioner and the County Education Officer of the area before embarking on your research. Failure to do that may lead to the cancellation of your permit.
2. Government Officer will not be interviewed without prior appointment.
3. No questionnaire will be used unless it has been approved.
4. Excavation, filming and collection of biological specimens are subject to further permission from the relevant Government Ministries.
5. You are required to submit at least two(2) hard copies and one (1) soft copy of your final report.
6. The Government of Kenya reserves the right to modify the conditions of this permit including its cancellation without notice.


**Director General
National Commission for Science,
Technology & Innovation**

Permit No : NACOSTI/P/16/41073/14091
Date Of Issue : 7th November, 2016
Fee Received :Ksh 1000



Figure D 1: Research clearance permit



**NATIONAL COMMISSION FOR SCIENCE,
TECHNOLOGY AND INNOVATION**

Telephone: +254-20-2213471,
2241349, 3310571, 2219420
Fax: +254-20-318245, 318249
Email: dg@nacosti.go.ke
Website: www.nacosti.go.ke
when replying please quote

9th Floor, Utalii House
Uhuru Highway
P.O. Box 30623-00100
NAIROBI-KENYA

Ref. No. **NACOSTI/P/16/41073/14091**

Date:
7th November, 2016

George Onyango Orido
Egerton University
P.O. Box 536-20115
EGERTON.

RE: RESEARCH AUTHORIZATION

Following your application for authority to carry out research on *“Exhaust gases energy recoverable from a diesel engine for maize grain drying,”* I am pleased to inform you that you have been authorized to undertake research in **Nairobi and Nakuru Counties** for the period ending **7th November, 2017.**

You are advised to report to **the County Commissioners and the County Directors of Education, Nairobi and Nakuru Counties** before embarking on the research project.

On completion of the research, you are expected to submit **two hard copies and one soft copy in pdf** of the research report/thesis to our office.


BONIFACE WANYAMA
FOR: DIRECTOR-GENERAL/CEO

Copy to:

The County Commissioner
Nairobi County.

The County Director of Education
Nairobi County.

The County Commissioner
Nakuru County.

COUNTY COMMISSIONER
NAIROBI COUNTY
P. O. Box 30623-00100, NBI
TEL: 341000

National Commission for Science, Technology and Innovation is ISO 9001:2008 Certified

Figure D 2: Research authorization letter